A Surface Water Model for the Orinoco river basin

Technical Report

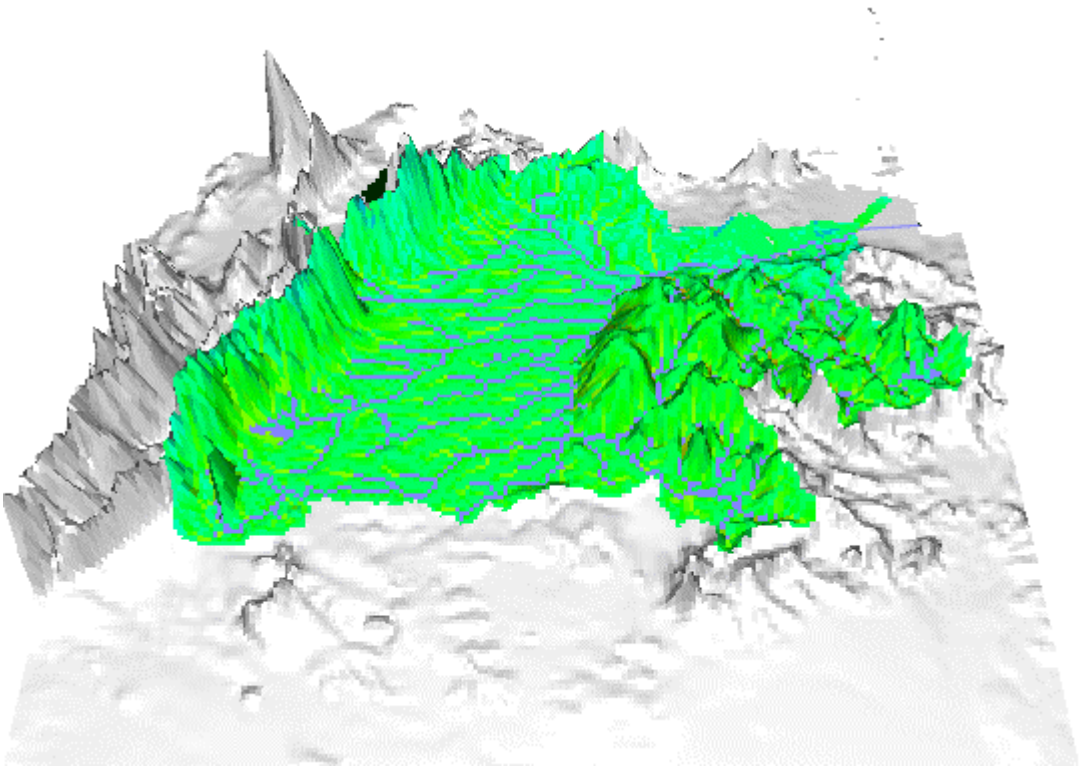

Utrecht University

P.P. Schot
A. Poot
G.A. Vonk
W.H.M. Peeters

A Surface Water Model for the Orinoco river basin

Technical Report

P.P. Schot
A. Poot
G.A. Vonk
W.H.M. Peeters

Utrecht, March 2001

Department of Environmental Sciences
Faculty of Geography
Utrecht University
P.O.Box 80.115
3508 TC Utrecht
The Netherlands
e-mail: p.schot@geog.uu.nl

Contents

List of figures

List of tables

1 Introduction

Conservation of freshwater ecosystems is one of the priorities of the World Wildlife Fund (WWF). To achieve this, WWF tries to develop solutions that integrate conservation with human needs. WWF is convinced that freshwater resources and ecosystems will only be conserved through management based on a *river basin approach*. This approach takes into account the landscape ecological relations which exist in the catchment. Such relations may be in the form of flowing water which transports the effects of interventions at one location to other locations in the river basin. Examples are the transport of pollutants by water downstream, the effects of dam construction on river water discharge and flooding dynamics downstream of the dam, etc. Such hydrological effects in turn have their effect on water-dependent ecosystems in the river basin. Examples are the negative effects of reductions in flooding area on the reproduction of fish species which need flooded areas for spawning, the fragmentation of habitat of water species through constructed dams which act as migration barriers, etc. Impairment of these ecological functions directly leads to problems for human communities which depend on these hydrological or ecological functions for their livelihood, e.g. fisherman, farmers, ecotourism operators, drinking water companies, industry, etc.

A recent example of the effort of WWF to integrate conservation with human needs is the Living Waters Campaign which started in 1999. The goal of this campaign is 'Ensuring that adequate fresh water is available, both now and in the future, for people and nature'. The targets of this campaign are to:

1. Implement action in at least five river basins demonstrating sustainable approaches to water management which balance long-term human uses and biodiversity conservation.
2. Increase, by 50 per cent, the area of the world's freshwater ecosystems that are newly committed for protection, restoration or effective management – commitments that include a total area in excess of 25 million hectares.

As part of target 1 WWF International has requested Utrecht University to develop a surface water model for the Orinoco river basin in South America. The purpose of the surface water model is to provide governments, NGO's and other stakeholders with a comprehensible tool for rough impact assessment of planned human interventions in the river basin on surface water runoff. The model may serve as a demonstration for other river basins of the need to have available such catchment wide tools to evaluate the possible effects of human interventions in one part of the river basin on water functions and water use by stakeholders in other parts of the basin. Depending on the needs expressed by the stakeholders in the river basin, the present hydrological model may be extended in future to include modules for impact assessment of different types of human intervention and land use change on relevant ecological and socio-economic functions.

This report describes the surface water model developed for the Orinoco river basin. In the next chapter hydrology and climate of the study area are presented. In the third chapter the general model concept is described. The fourth chapter describes the effects of various processes in the model on the model results, resulting in the choice of a model with least complexity and maximum efficiency. In the fifth chapter, calibration and verification of the chosen model are discussed. The possibilities and limitations of the model are described in the sixth chapter. The final chapter contains a short evaluation and recommendations for possible future improvements of the model.

2 Study area

2.1 General description

The Orinoco river basin is located in the South American countries Venezuela and Colombia. The river Orinoco is the third largest river in the world. It's total length measures 2140 km and drains an area of 830,000 km^2 (MacKee et al, 1989; Stallard et al, 1990; Rawlins, 1999). The Orinoco River has it's origin on the southern end of the Guyana Highlands and flows from there around this shield and northwards towards the Atlantic Ocean (figure 2.1). On its course many tributaries join the stream, most of which have their origin in the Andes mountains and flow from there over the low lying Llanos (the Spanish word for plains), towards the Orinoco main stream.

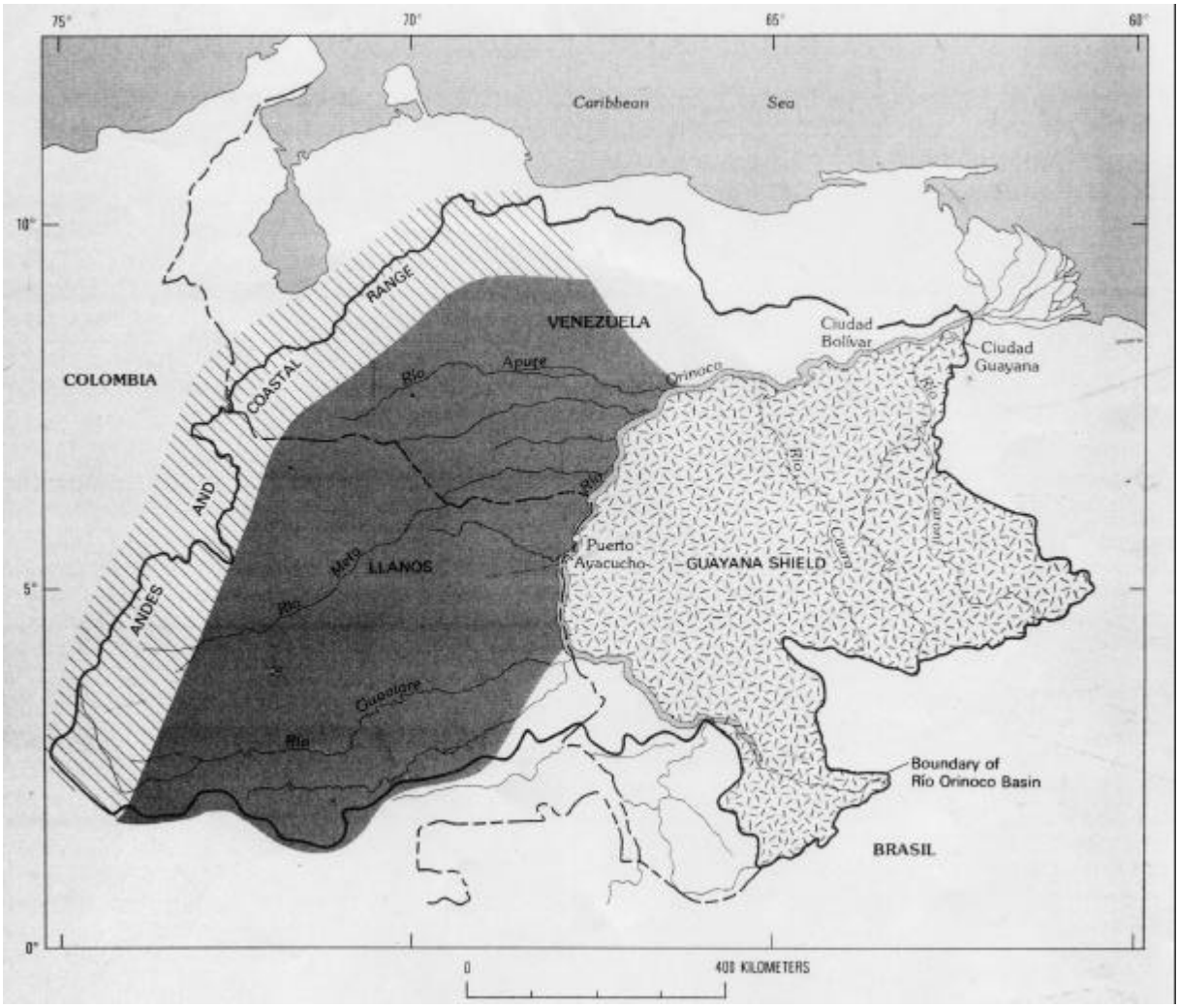

Figure 2.1 The basin of the Orinoco River (Source: MacKee et al, 1989).
The solid line encloses the drainage area. The shaded areas distinguish the three geographical zones: Andes, Llanos and Guayana Shield.

2.2 Climate

The Orinoco basin has a tropical climate. Two seasons can be distinguished. The seasons are marked by rainfall differences rather than by temperature changes (Rawlins, 1999). Average daily temperatures in the Llanos do not vary greatly from the annual mean of 27 to 30 degrees Celsius. The rainy season extends from about April to November. The dry season is from

December through March. Annual precipitation ranges from about 1 meter in the North to about 4 meters in the Southern part of the basin.

An analyses of the basins precipitation and temperature patterns was made on the basis of data from the CRU Global Climate Dataset (New et al, 1998). In this dataset, measured climatic data of a large number of measuring stations worldwide have been collected and interpolated to cover a grid of 0.5 * 0.5 degrees. The distance between temperature measuring stations was sufficiently small to ensure significance of inter-station correlation for the whole time series in the Orinoco basin. For precipitation this is only true for the period after 1961 (New et al, 1998). Most of the climatological measuring stations are located in the Andes mountains. Only a few stations are located on the Llanos and in the Guyana Highlands.

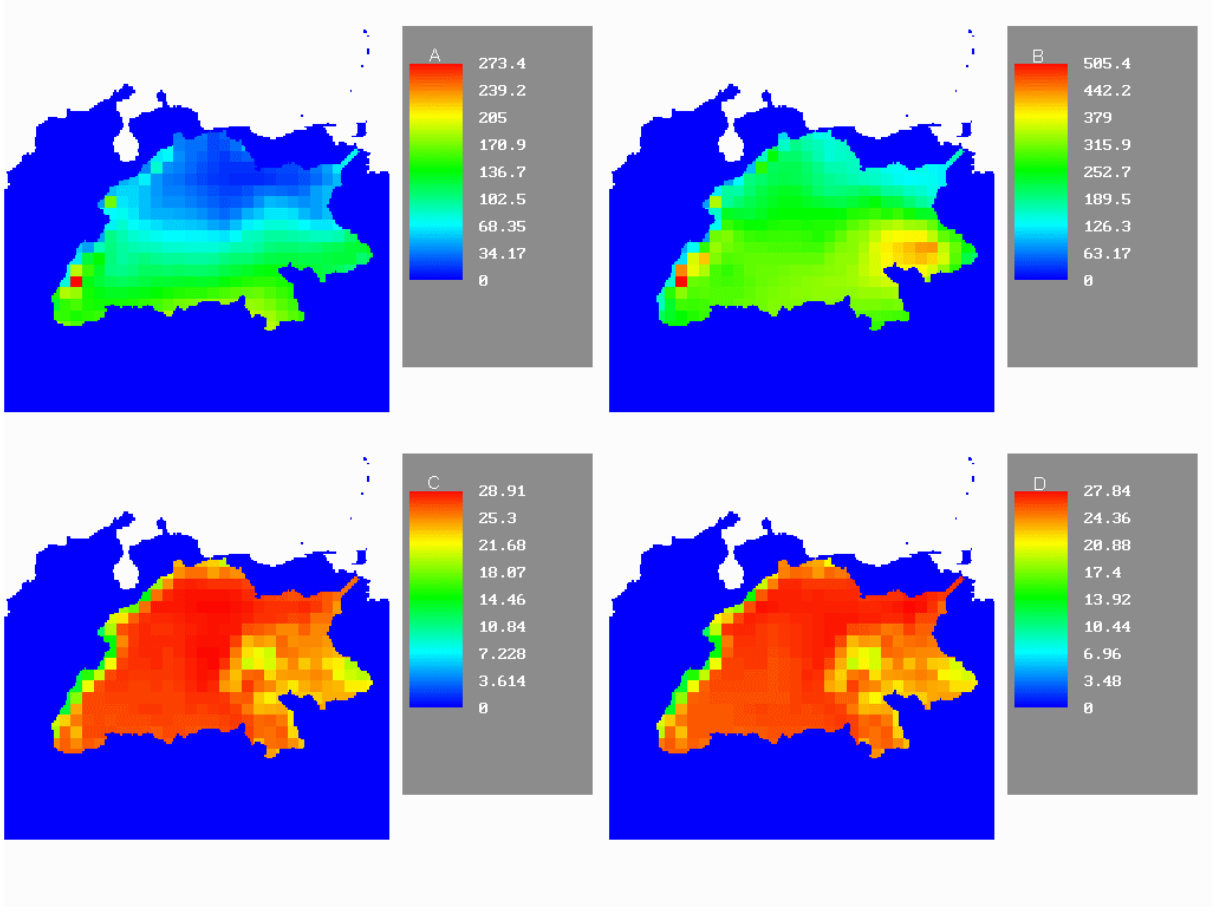

Figure 2.2 Mean monthly precipitation in mm and temperature in degrees Celsius during the dry and wet season.
A represents mean monthly precipitation during the dry season (December-March);
B represents mean monthly precipitation during the rainy season (April-November);
C represents mean monthly temperature during the dry season (December-March);
D represents mean monthly temperature during the rainy season (April-November).

Figure 2.2 shows mean monthly precipitation and temperature for dry and rainy season in the Orinoco basin, as derived from the CRU dataset. These figures confirm the patterns described in literature. Furthermore spatial variation of precipitation and temperature can be derived from these figures. Precipitation figures show high precipitation on the Guyana Highlands and the Andes. Precipitation is higher in the Southern part of the basin than in the Northern part. Temperatures are more or less constant during the year, a little lower during the rainy season than during the dry season. Temperature variance is mostly caused by elevation differences.

2.3 Hydrology

The average water discharge of the Orinoco River to the delta just below the Caroni River at Cuidad Guayana, is about 36,000 m^3/s (MacKee et al, 1989). This makes the Orinoco River the third largest river in the world in flow, discharging into the ocean. Variation in river discharge is large. Daily means have been measured reaching from 1,050 m^3/s to 82,100 m^3/s at Musinacio hydrographic measuring station, which is located near the outflow point of the Orinoco River. Besides a large variation in river discharge, the variation in river water level is also large. Large areas in the Orinoco basin are inundated during wet periods. Historical records of the stage at measuring station Musinacio in the Orinoco main stream (fig. 2.4) show differences in stage of about 17 meters between low flow and high flow.

Most of the large tributaries of the Orinoco, such as the Apure, Meta and Guaviare River, have their origin in the Andes mountains and join the Orinoco from the western side. Several other large tributaries, such as the Caura River and the Caroni River have their origins on the Guyana Highlands and join the Orinoco from the eastern side. The mean contribution of large tributaries to the discharge of the Orinoco is presented in figure 2.3. A peculiarity of the Orinoco River is that it divides its water into two streams in the south of the basin near its origin. One of the streams continues as the Orinoco and the second stream, known as the Casiquiare channel, discharges into the Amazone basin. The strict hydrological separation between different watersheds that is usually found therefore does not apply here.

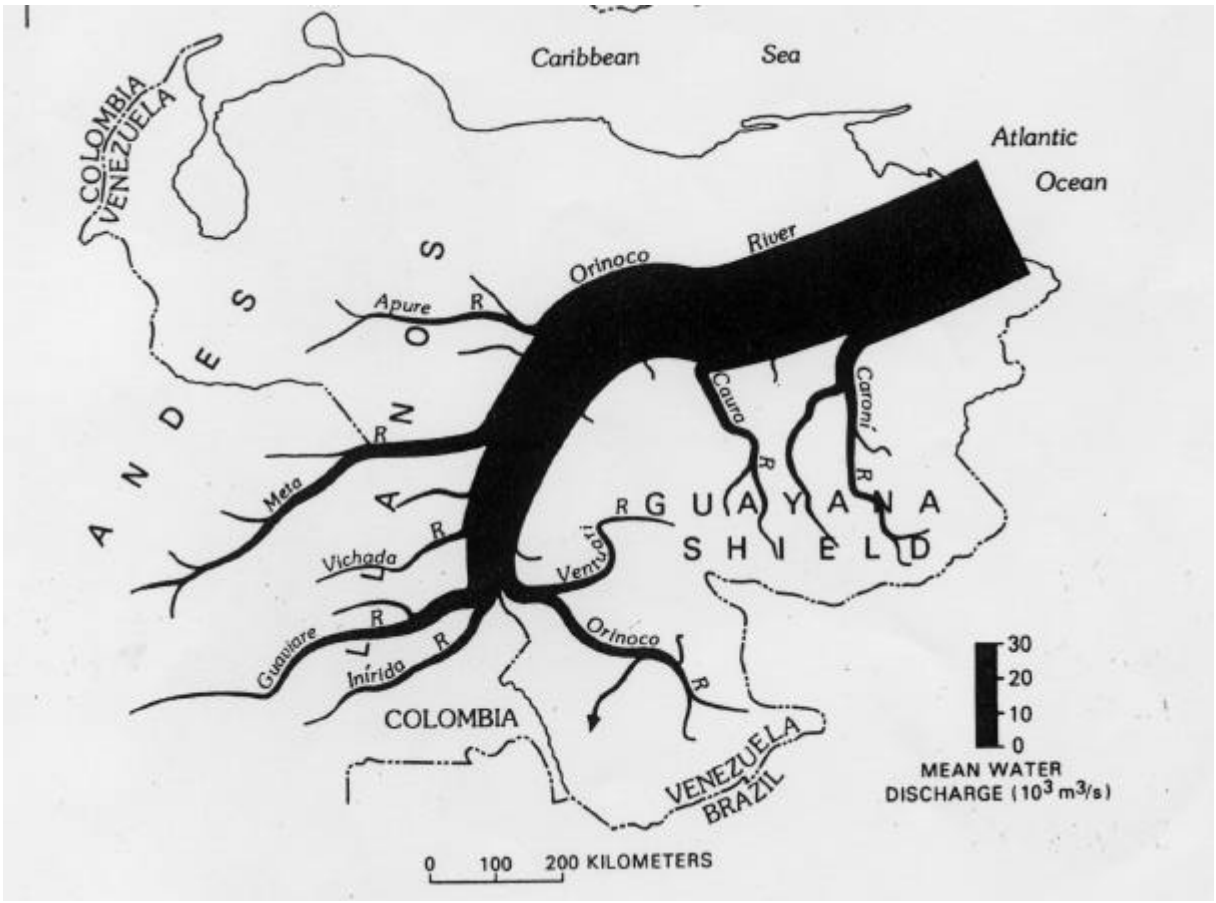

Figure 2.3 Mean discharge in the Orinoco river basin (Source: Meade et al, 1990). Width of river patterns indicates the quantity of mean discharge.

In this study an analysis of river discharge was made on the basis of discharge data from the Global Runoff Data Centre in Germany, the Ministerio del Ambiente y de los Recursos Naturales in Venezuela and the Instituto de hidrologia meteorologia y estudios ambientales in Colombia (appendix I). Discharge data has become available for a considerable number of hydrographical measuring stations. However, for only a few stations discharge time series were longer than a few years. On the basis of the length of the time series and the location in the river basin, a selection was made of stations to include in this study (figure 2.4).

The longest and complete time series of monthly discharge from 1925 to 1990 was available for the Venezuelan station Puente Angostura, located near the end of the main river channel before it dissipates into the Orinoco coastal delta. In this study Puente Angostura measuring point is considered to reflect variation in river discharge at the outflow point.

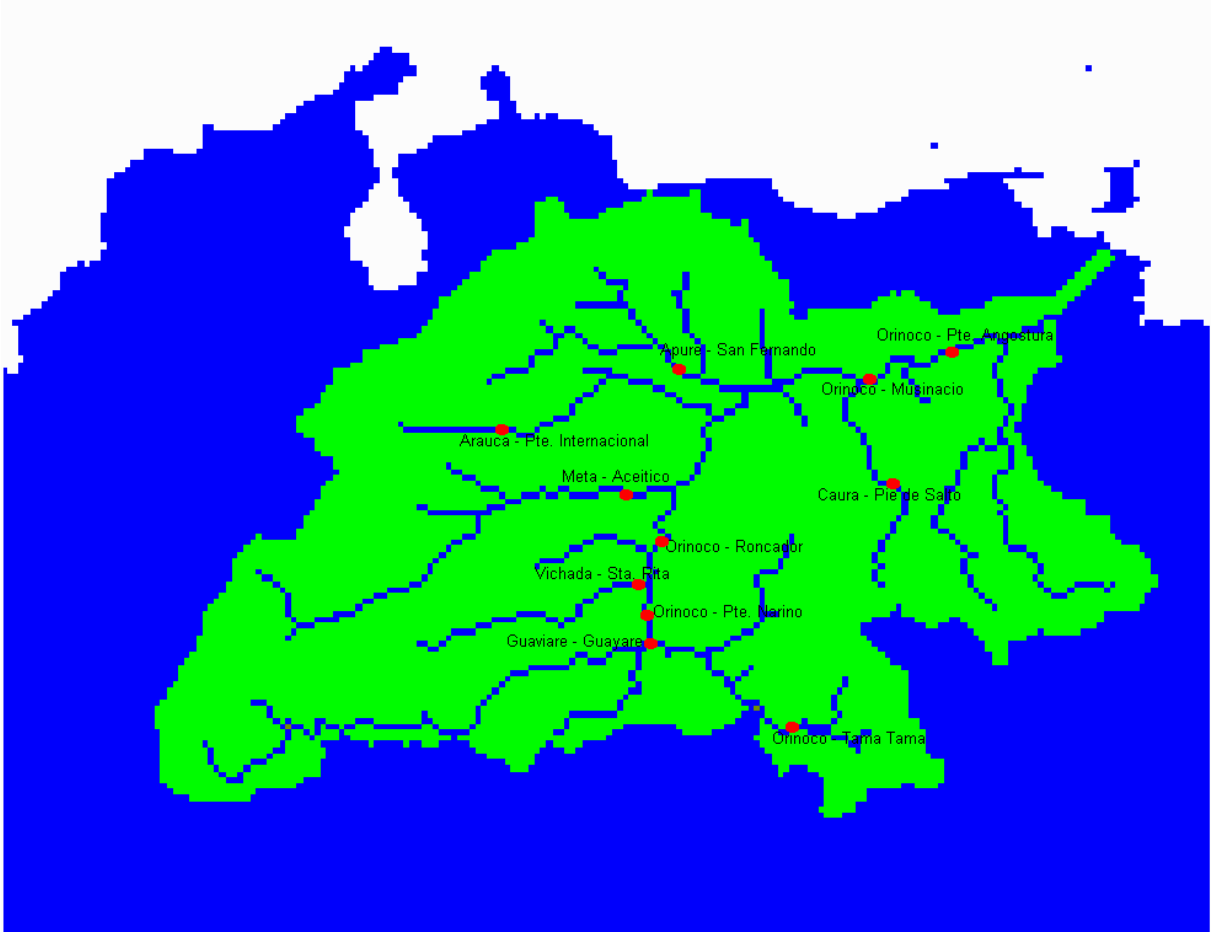

Figure 2.4 Hydrographic measuring stations in the Orinoco river basin included in this study.

Figure 2.5 reflects the yearly variation in monthly averaged river discharge at Puente Angustura. A sinusoid form of the hydrograph can be distinguished with periods of relatively high and low discharge reflecting discharge variation as determined by the rainy and dry seasons.
Figure 2.6 shows a flow duration curve for Puente Angostura measuring station. The figure is a cumulative distribution function, showing chances of occurrence of a discharge lower than a specific value, assuming normally distributed discharge values. The large variation in monthly discharge found in literature is reflected in this figure.

Figure 2.7 shows the variation in yearly total discharge at Puente Angostura from 1925 to 1990. The average yearly discharge of this period is also shown. Periods of high and low discharge can be distinguished from this figure.

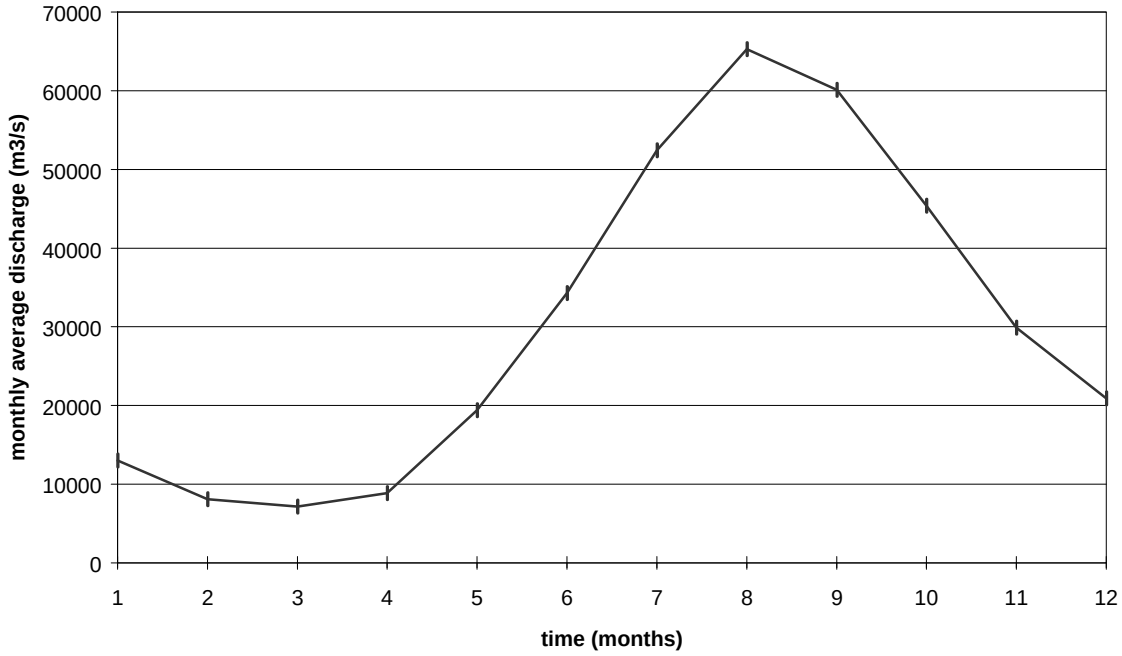

Figure 2.5 Temporal variation in monthly averaged river discharge at Puente Angostura (1925-1990).

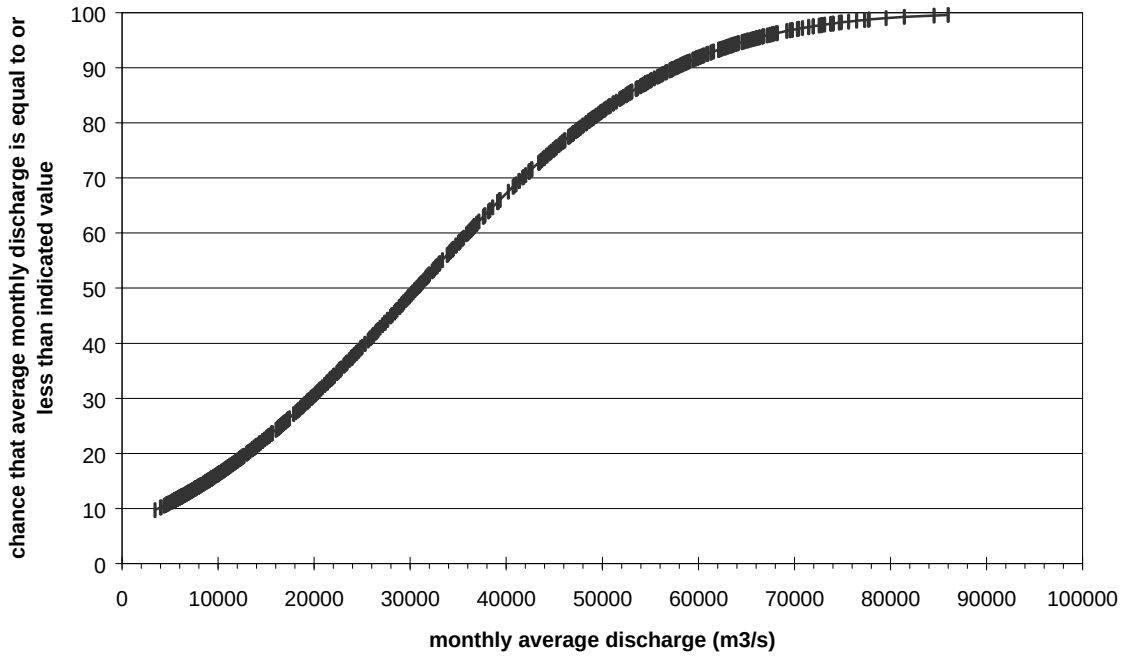

Figure 2.6 Flow duration curve for Puente Angostura measuring station (1925-1990).
The curve is a cumulative distribution function, showing the chance that monthly discharge is equal to or less than a value that is indicated on the discharge axis, assuming normally distributed discharge values.

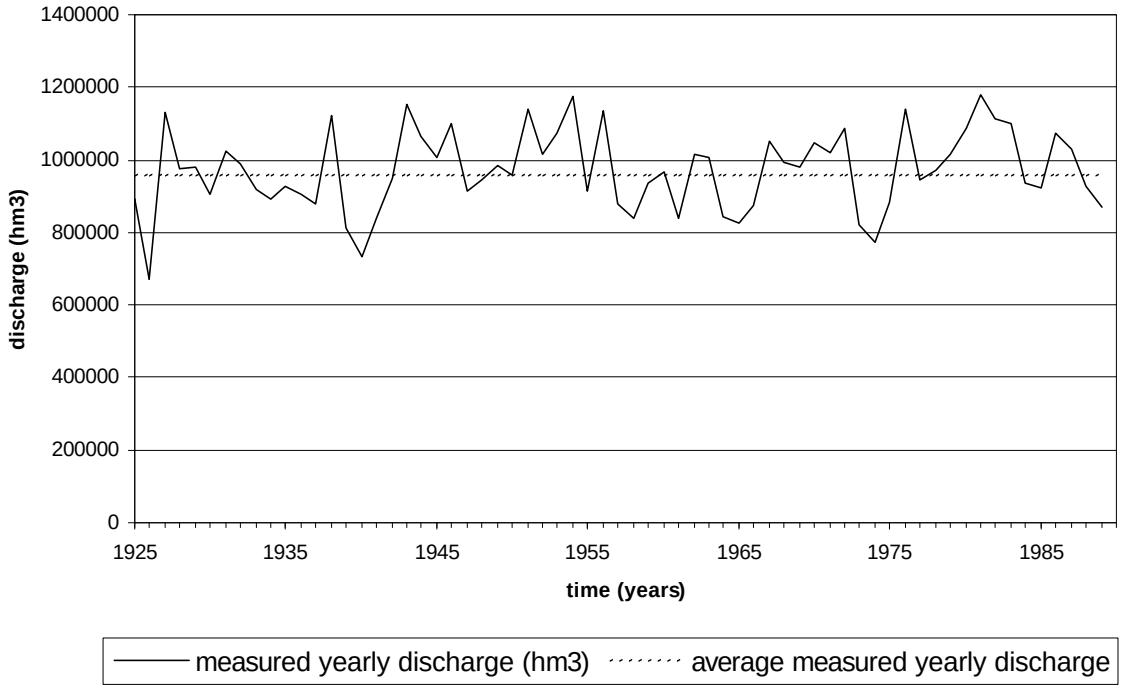

Figure 2.7 Long term yearly total discharge at Puente Angostura and 65-year average discharge (1925-1990)

3 General model description

3.1 Model concept

The hydrological cycle of a drainage basin can be viewed as a series of storages and flows. A water balance is often used as a framework to describe the transformation of input (precipitation) through this cycle. The algorithms to describe the different flows through the compartments may differ from completely empirical to more conceptual, depending on how much consideration is given to the physical processes acting on the input variables to produce the outflow (Kwadijk, 1993). During the last decades many models have been developed that describe the transformation of precipitation into runoff for river basins. However, many of the existing models require large data sets, detailed both in space and in time. Even in densely monitored areas, data for many of the parameters are only available at a very low spatial resolution. To overcome this problem, Van Deursen and Kwadijk (Kwadijk, 1993; Deursen, 1995) developed a water balance model that requires relatively little input data and can be applied to large river basins.
This model has been successfully applied to the basins of the river Rhine (Kwadijk, 1993), the Yangtze and the Ganges-Brahmaputhra (Deursen and Kwadijk, 1994). For this reason, and because few data was available, this model concept was chosen to model the large basin of the Orinoco River.

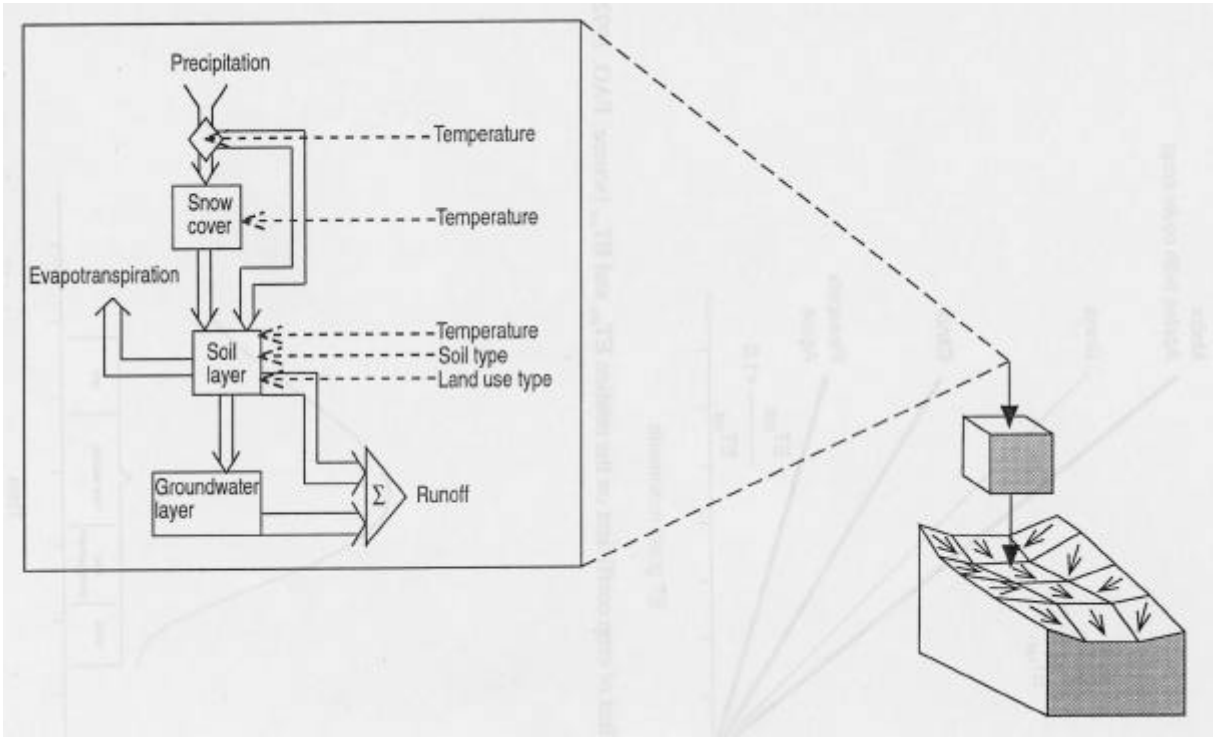

Figure 3.1 Flow diagram of the Orinoco surface water model concept .

In the model of Van Deursen and Kwadijk, the water balance consists of three storages (figure 3.1):

- snow
- soil water
- groundwater

These storages are connected by six fluxes:

- precipitation

- snowmelt
- evapotranspiration
- groundwater recharge
- rapid runoff
- delayed runoff

On these fluxes act five controls:

- temperature
- maximum water storage capacity of the soil (or soil type)
- crop coefficient (or land use type)
- separation coefficient
- recession coefficient

The snow storage gains water from precipitation and looses water by snowmelt. Both fluxes are controlled by temperature. The soil water storage gains water from infiltration of precipitation. It looses water through the evapotranspiration flux, which is controlled by temperature and the maximum water storage capacity of the soil, which in turn is a function of soil type. The amount of effective precipitation (i.e. precipitation – evapotranspiration) is separated into a flux of soil water to the groundwater storage, groundwater recharge, and rapid runoff by the so-called separation coefficient. The groundwater storage gains water from groundwater recharge and looses water to the delayed runoff. This last flux is controlled by the so-called recession coefficient. Storages, fluxes and controls are described in more detail in section 3.2.1

The model approach assumes that the water balance on a location only depends on local conditions from the previous time step. Water excess at one location is assumed not to contribute to the water balance of other locations. For example, overland flow at one location is not expected to contribute to the water balance of locations/cells downstream, for instance as a supply to infiltration in downstream locations. Another assumption of the model approach is that all runoff is assumed to leave the basin within one model time step.
A time step of one month was considered to be sufficiently long to ensure this assumption in previous studies by Kwadijk and Van Deursen. Assuming an average surface water flow velocity of 1 m/s, a distance of approximately 2700 km is travelled within one month. Considering the length of the Orinoco River, 2140 km, one month is assumed in this study to be sufficient to let all surface water in the main streams of the Orinoco and its tributaries reach the basin outlet. For water stored on floodplains and other water not accounted for in the calculation of the groundwater storage it can be doubted if this water reaches the outflow point within the same month as it developed as runoff. Besides this, no matter how large the time step, precipitation falling at the end of a time step is (at least for the rapid runoff part) considered as discharge for that time step, while in reality this amount of precipitation is likely to come to discharge within the next time step. Despite these limitations, experiences with the one-month time step were satisfying in previous studies in other large river basins comparable in size to the Orinoco. Therefore a time step of one month was chosen for the model of the Orinoco basin.

The mentioned fluxes, storages and controls vary spatially. To take this spatial variation into account, model variables and parameters are stored in a raster Geographical Information System. The basic software used is PCRaster which is a raster GIS that has been extended with a set of general tools that may be used to build spatially distributed models, amongst others hydrological models. With these tools water balances may be modelled and calculated for each of the cells of the raster system.

Stream flow or runoff in the river basin is calculated on the basis of the rapid runoff flux and the delayed runoff flux calculated from the water balance calculation in each raster cell for each time step. For each grid-cell these fluxes are drained towards the lowest neighbouring cell by geomorphological routing. For this routing a digital elevation model (DEM) is used from which the Local Drainage Directions (LDD) are determined. By subsequently following the direction towards the lowest neighbour, the flow path of runoff towards the outlet of the basin is established (Kwadijk, 1993). The accumulation of fluxes per cell provides a simulation of runoff per time step. This procedure is described in more detail in section 3.2.2.

3.2 Model input

3.2.1 Water balance input

To calculate the water balance per cell, the following model input is needed:

- precipitation
- temperature
- maximum water storage capacity of the soil
- crop coefficient
- separation coefficient
- recession coefficient

All data sources that were used are described in appendix I.

Precipitation and Temperature
Time series of precipitation and temperature values, covering the Orinoco basin on a 0.5*0.5 degree basis, were derived from the CRU Global Climate Dataset (New et al, 1998) described in the second chapter. The measured values in this dataset are already spatially interpolated between the meteorological measuring stations and correction of temperature and precipitation with elevation has been accounted for.

Maximum water storage capacity of the soil
The maximum water storage capacity of the soil in the model is defined as the difference of soil water content between field capacity and wilting point. Information on this was derived from a dataset by Batjes (Batjes, 1996). This dataset contains derived soil properties, among which a parameter named available water capacity (AWC) on a 0.5*0.5 degree grid. It is assumed that average rooting depth within the Orinoco basin equals 1 meter. Therefore the maximum water storage capacity of the soil in the Orinoco model is set equal to the AWC for one meter soil depth as derived from Batjes (1996). The used map with maximum water storage capacity of the soil is presented in figure 3.2.

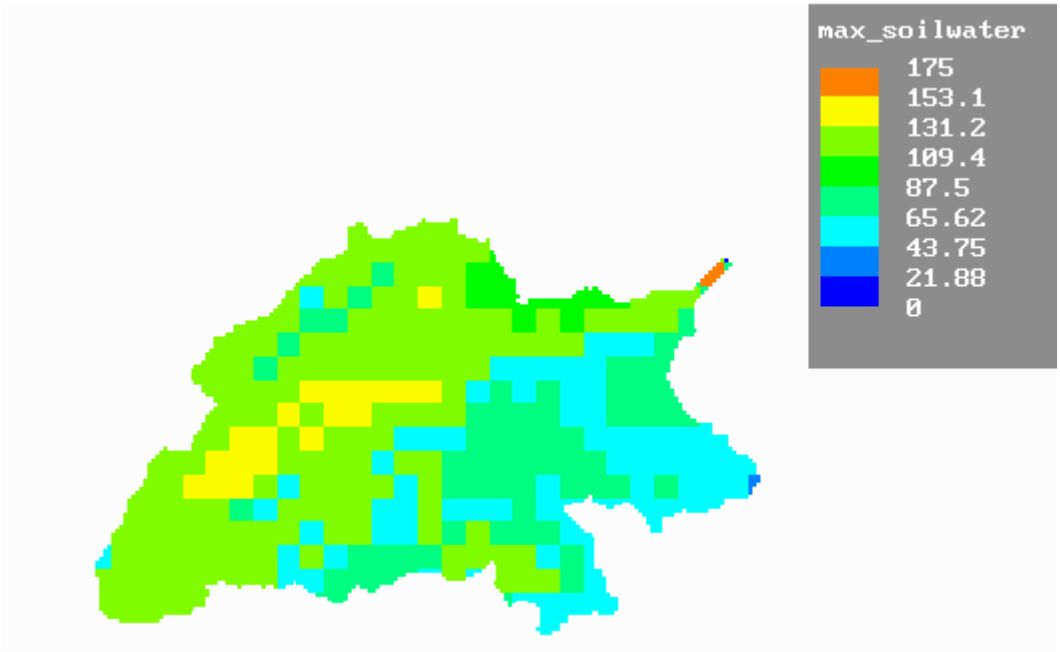

Figure 3.2 Maximum water storage capacities of the soil in mm in the Orinoco basin.

Crop coefficient

Crop coefficients are assigned on the basis of land cover characteristics. A land cover map was abstracted from the Global Land Cover Characterisation (GLCC) database version 2.0 (figure 3.3). GLCC is a global 1 km resolution land cover dataset available at U.S. Geological Survey's (USGS) EROS Data Centre. A land cover map was used that had been classified according to the USGS Land Use/Land Cover System (Anderson et al, 1976) . It appeared that the Orinoco basin consisted, according to the dataset, for more than 95% of only two land cover classes: evergreen broadleaf forest and savannah. It was decided to filter all other minor land cover classes out. Filtering these minor classes out can be justified since considering the purpose of the map in the model, no dramatic model improvements are to be expected from including the minor land cover classes. This is true since the minor land cover classes were either covering an insignificant area, or they were unsuitable to be used as model input as they are mixtures of many totally different crop types. Examples of this are land cover classes named cropland/grassland mosaic and cropland/woodland mosaic. A suitable single crop coefficient to assign to these mixtures of land cover types in order to calculate evapotranspiration cannot be found in literature. Literature crop coefficients of single crops can only be extended to land cover classes if the majority of the land cover within a cell equals this crop type or a crop type with comparable evaporative characteristics. Such data however were not available. Crop coefficients used in the model were derived from Van Deursen and Kwadijk, 1994. From their data it appeared that both of the distinguished land cover classes, evergreen broadleaf forest and savannah, were assigned a crop coefficient of 1,1. This value of 1.1 was used as crop coefficient for both land cover classes in this study. The modified land cover map is presented in figure 3.4.

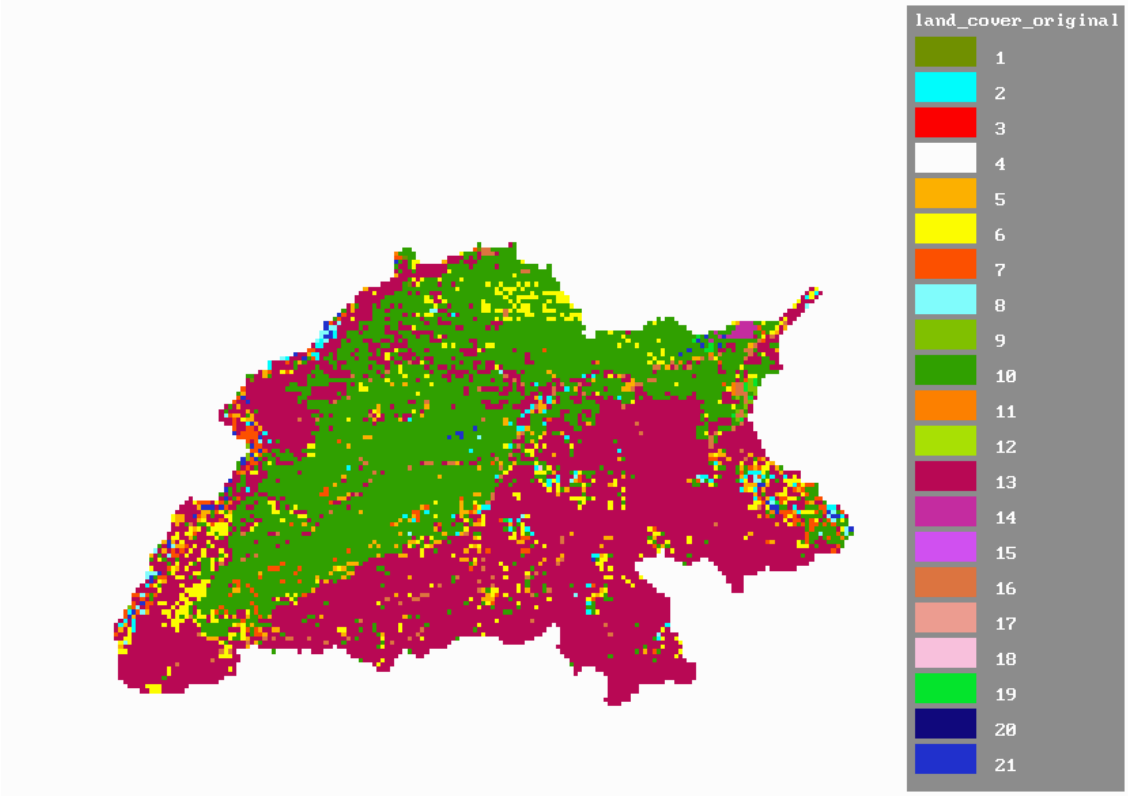

Figure 3.3 Land cover map of the Orinoco basin derived from the GLCC-database.
Classes are the following: 1. urban and built up land; 2. dryland cropland and pasture; 5. cropland/grassland mosaic; 6. cropland/woodland mosaic; 7. grassland; 8. shrubland; 9. mixed shrubland/grassland; 10. savannah; 11. deciduous broadleaf forest; 13. evergreen broadleaf forest; 14. evergreen needleleaf forest; 16. water bodies; 18. wooded wetland; 19. barren or sparsely vegetated; 21. wooded tundra.

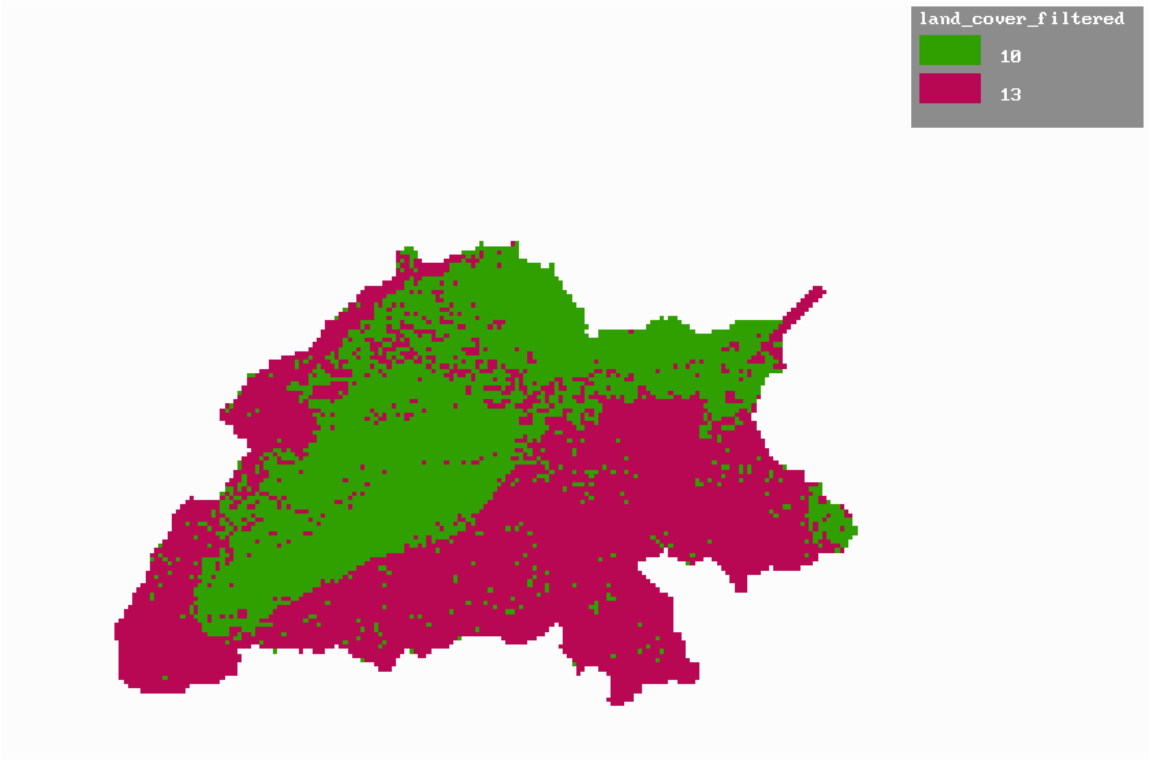

Figure 3.4 Pre-processed land cover map of the Orinoco basin, based on figure 3.3.
Minor land cover classes and combination land cover classes were filtered out. Remaining classes are: 10. savannah; 13. evergreen broadleaf forest.

Separation and recession coefficient
The separation and recession coefficients are empirical model parameters. These coefficients were used for calibration (see chapter 5). Although physical backgrounds for variation of these coefficients can be found, a single value of the separation coefficient and the recession coefficient has been applied for whole river basins in past studies by Kwadijk and Van Deursen.

3.2.2 Routing input

The runoff calculated from the water balance of each cell is accumulated and routed towards the outflow point, with a digital elevation model. Before accumulation, runoff from each cell in mm is converted to a runoff volume by multiplication with cell area. The area of each cell was calculated assuming the earth is a complete sphere with a radius of 6378137m.

A digital elevation model from the GTOPO30 dataset, released by U.S. Geological Survey's EROS Data Centre was used in this study (appendix I). GTOPO30 is a global digital elevation model with a horizontal grid spacing of 30 arc seconds (approximately 1 km). Considering the size of the Orinoco basin and the detail with which measured data is known, a cell size of 5 arc minutes, which is approximately 10*10 km on the equator was chosen as cell size for the Orinoco basin model (figure 3.5). The GTOPO30 elevation map of the basin and all other base maps of the model were resampled to this resolution and reprojected to the projection of the elevation map (geographic projection).

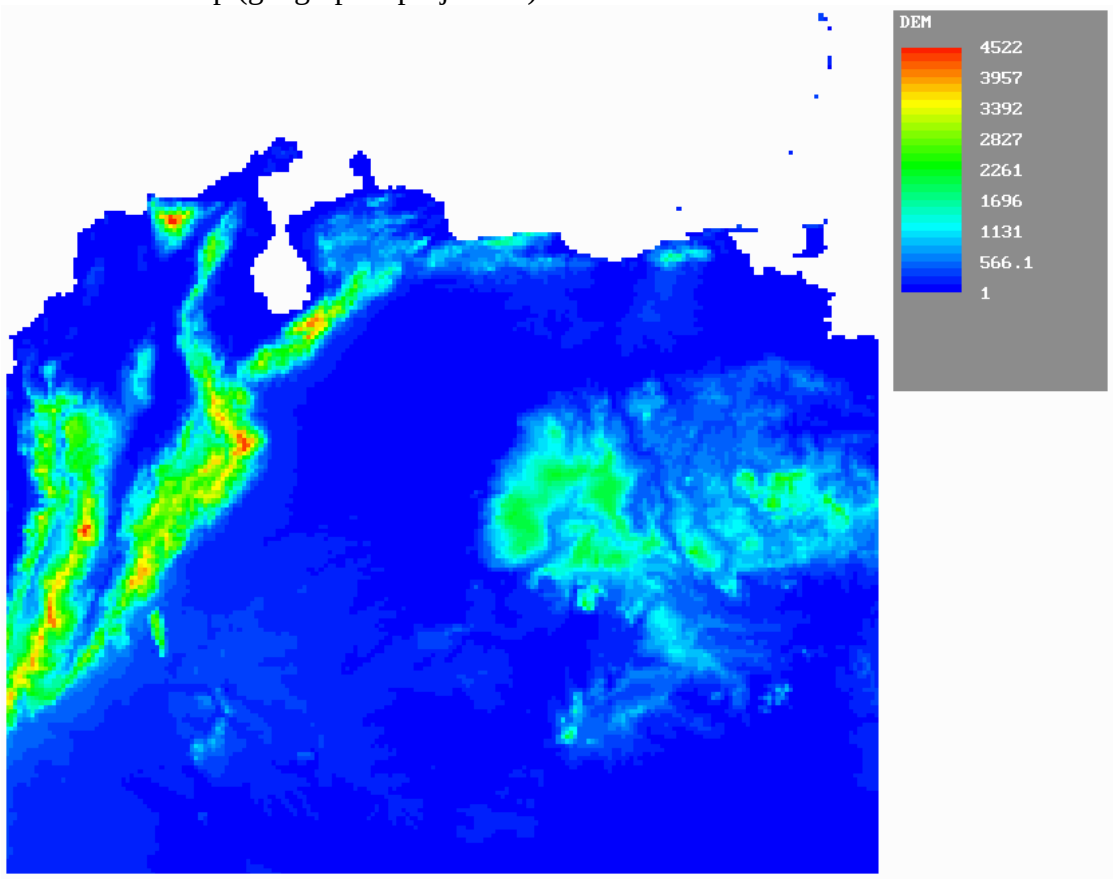

Figure 3.5 Digital elevation model (DEM) of the area in which the Orinoco basin is located. Elevation in meters.

In the routing process each grid-cell drains towards the lowest neighbouring grid cell, and by subsequently following the direction towards the lowest neighbour, the flow path of runoff

towards the outlet of the basin is established (Kwadijk, 1993). A map with local drainage direction (LDD) was calculated by derivation of the digital elevation model (figure 3.6).

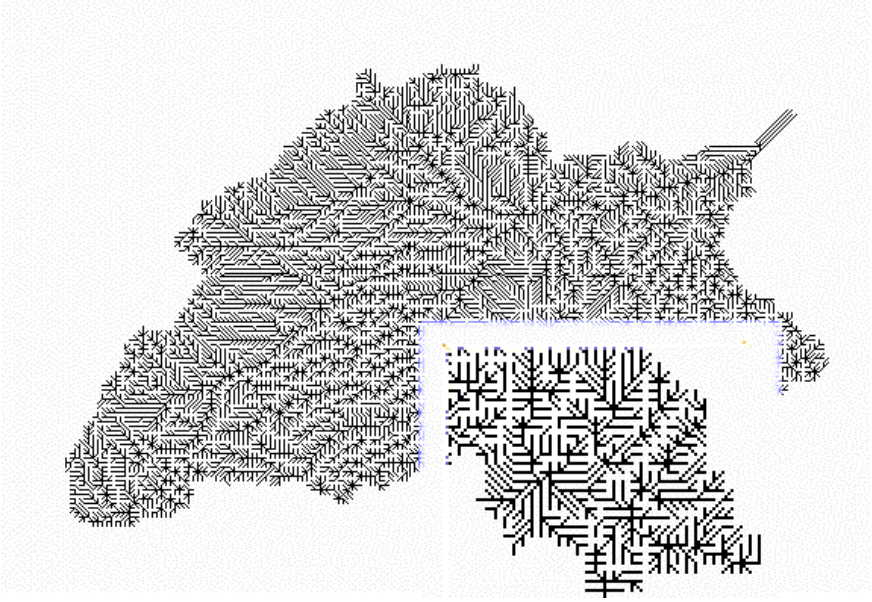

Figure 3.6 Map with local drainage directions (LDD) in the Orinoco basin.
The south-eastern part has been enlarged to show the structure of the drainage network.

The original LDD map did not represent the boundaries of the Orinoco basin and the river network correctly (figure 3.7). Therefore it was modified by adjusting the DEM. The resulting basin boundary and river network of the LDD map after modification is presented in figure 3.8.

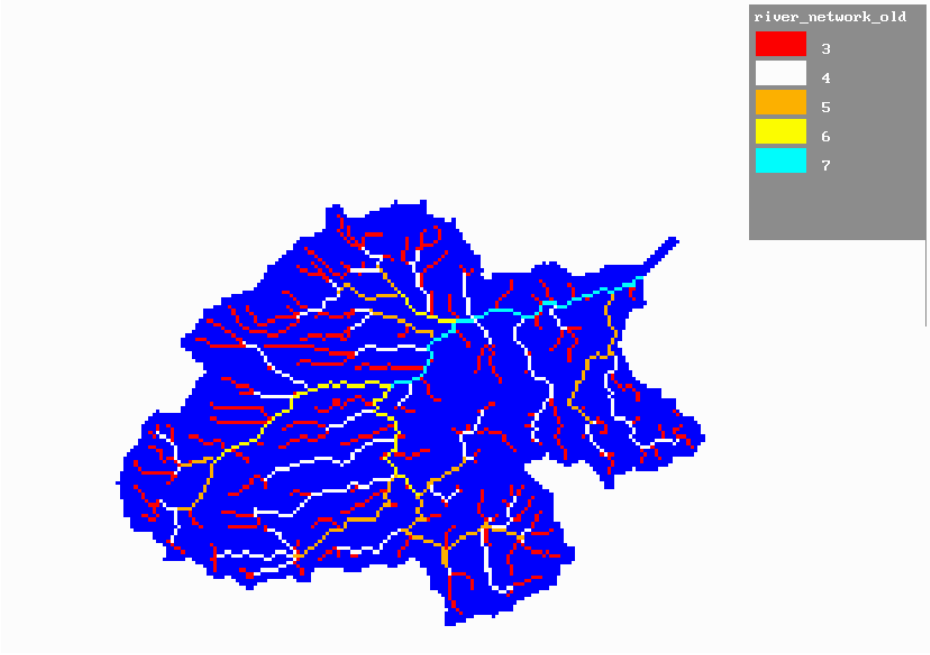

Figure 3.7 Stream order network according to the Strahler classification and basin boundaries of the Orinoco basin before modification of the digital elevation model.
The first two orders are not shown.

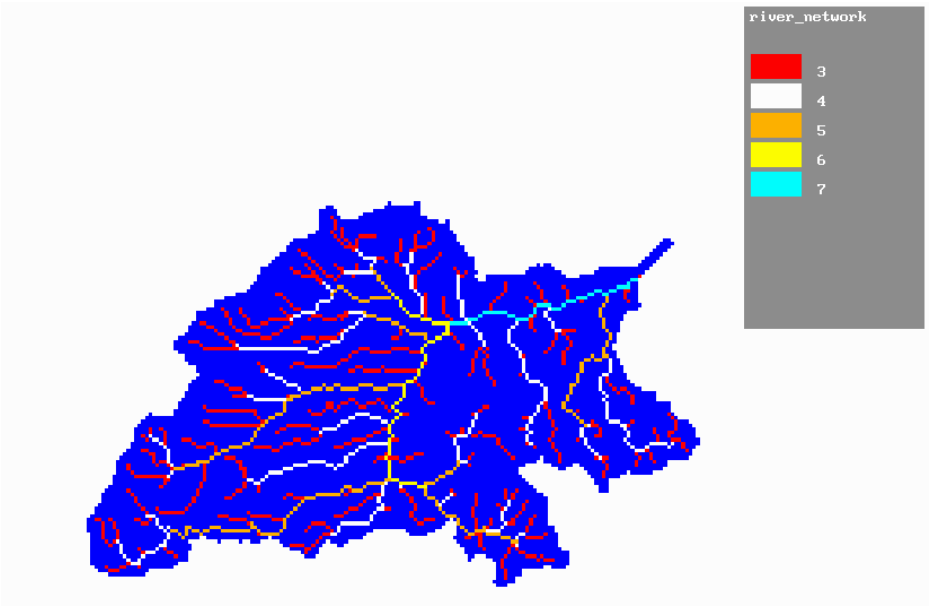

Figure 3.8 Stream order network according to Strahler classification and basin boundaries of the Orinoco basin after modification of the digital elevation model.
The first two orders are not shown.

3.3 Model output

During simulations, all fluxes and storages can be written to output time series and maps. An output time series reflects development of a flux or storage in time on a number of specified locations. An output map represents the spatial distribution of a flux or storage. Output maps can be generated for specified time steps during a simulation. Time series of maps can be generated to show development of fluxes and storages in space and time.

4 Model components

4.1 Method of model selection

Models describing parts of the hydrological cycle usually consist of storages and fluxes. In a simple model only a few processes in this cycle are described in a simple way. When there are more processes added to a model and/or processes are modelled in a more detailed way, the model complexity increases as does the amount of input data needed. A more complex model doesn't necessarily give better results (Perk, 1996). Therefore, the effect of the various processes that are described in the model of Van Deursen and Kwadijk have been explored for the Orinoco surface water model. This was done by starting with the most simple model: precipitation falls on an 'impermeable soil' and flows as overland flow over the ground surface towards the outlet of the basin. Step by step another flux and/or storage was added to the model and the effects on the model results were determined in a qualitative way. In the first step a snow storage was added to the model. In the second, third and fourth step, evapotranspiration was modelled in three different ways. In the fifth step a groundwater storage was added. In the sixth step, a flux of water which is lost from the basin towards the Amazon basin via the Casiquiare channel was added. On the basis of the results obtained with the various models, one final model was selected.

4.2 Precipitation

The first and simplest model of which performance was explored in this study consisted of precipitation falling on a surface. The precipitation falling in the basin area is directly converted to runoff and accumulated as discharge by routing it over the DEM towards the outlet of the basin. This model consists of only two fluxes and no storages. Precipitation is converted to discharge without any losses and/or delays. The following equation describes the water balance at location x, y at time step t.

$$R_{x,y,t} = P_{x,y,t}$$

R = runoff (mm)
P = precipitation (mm)

Discharge at a given location is generated from runoff by accumulation of runoff generated by the upstream cells. The discharge in m^3/s in a basin per time step is calculated by:

$$Q = \left(\frac{\sum (Runoff * 1000 * Cell\ area}{Seconds\ per\ month} \right)$$

Q = discharge in the basin (m^3/s)
Runoff = total runoff from a cell in a time step, sum of rapid and delayed runoff (mm)
Cell area = area of cell as described in paragraph 3.2.2 (m^2)
Seconds per month = number of seconds per month (s)

The model runs were made with monthly averaged input precipitation data of the time period from 1965 to 1995. As no storages are present in the model, the initial situation was equal to the equilibrium situation. A model run was made calculating average monthly discharge occurring during each month resulting from input average monthly precipitation. The

discharge in the equilibrium situation for each month in an average year on Puente Angostura is presented in figure 4.1.

From qualitative interpretation of figure 4.1 it becomes clear that simulated monthly averaged discharge values exceed average measured monthly discharge values during the greater part of the year. Furthermore, in the simulated situation, more water comes to discharge than in the measured situation. This may be a result of neglection of losses and delays in the simple precipitation model.

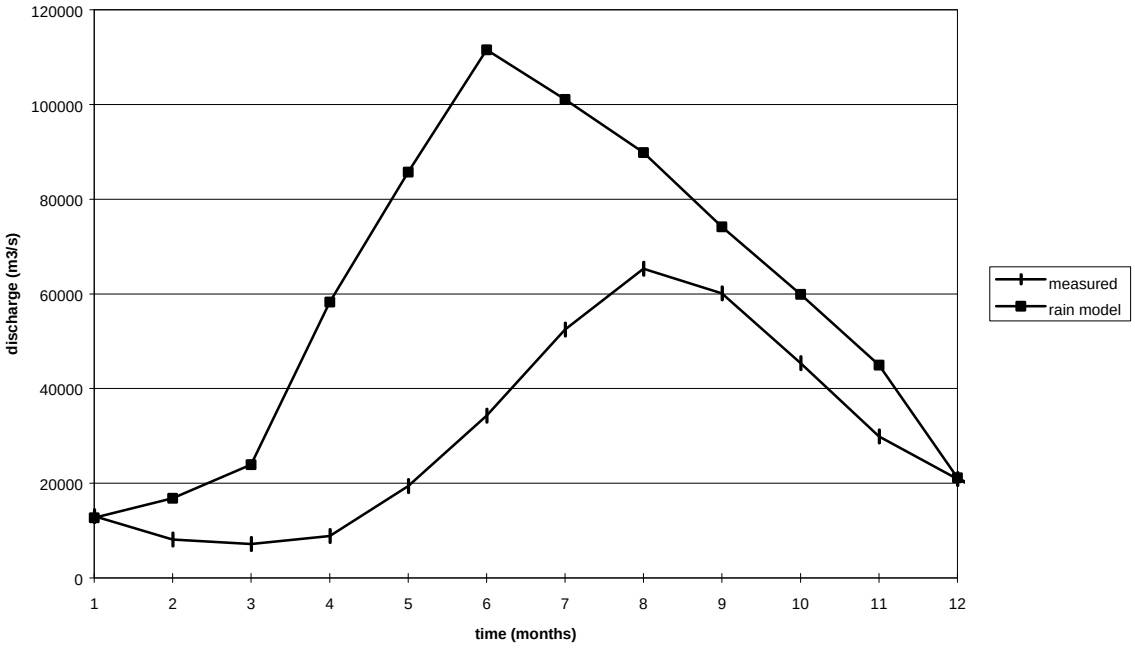

Figure 4.1 Monthly averaged measured and simulated discharge of the model with direct generation of discharge from precipitation.

4.3 Snow

The second model includes a storage for snow in the basin area. The following equation describes the water balance at location x, y at time step t according to this model.

$$R_{x,y,t} = P_{x,y,t} + dS_{x,y,t}$$
$$S_{x,y,t} = SNS_{x,y,t}$$

R = runoff (mm)
P = precipitation (mm)
dS = change in water volume stored (mm)
SNS = amount of water stored in the snow cover (mm)

Discharge is generated from runoff in a similar way as for the first model.

In paragraph 3.1 it was already explained that both the formation and the melting of snow is controlled by temperature. When the temperature is below a critical temperature, all

precipitation falling on a certain location, is assumed to be snow. When the temperature is higher than the critical temperature, snow melts according to the following formula:

$$Q_s = (T_m - T_0) * c_0 \left(\frac{L}{t^{-1}} \right)$$

in which

Q_s = the snow melt flux ($L*t^{-1}$)
T_m = the average daily temperature (K)
T_0 = a critical temperature above which snow-melt starts (K)
c_0 = the melt rate per degree Celsius ($L*K^{-1}*t^{-1}$)

In this study a critical temperature of zero degrees Celsius and a melt rate of 18 mm per degree Celsius per month was used.

The model runs were made with monthly averaged input temperature and precipitation data of the time period from 1965 to 1995. The model was run until an equilibrium situation of the snow storage was reached on yearly basis.

The discharge in the equilibrium situation for each month in an average year on Puente Angostura is presented in figure 4.2, together with the discharge in the equilibrium situation for the first model.

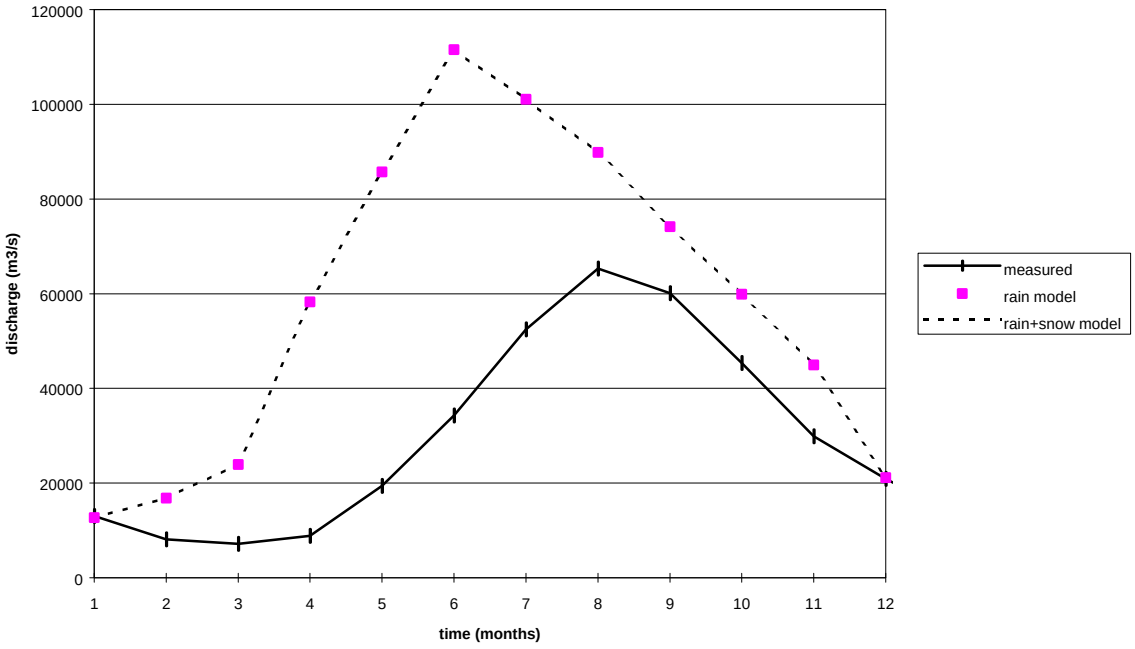

Figure 4.2 Monthly averaged measured and simulated discharge of two models.
Added in comparison with figure 4.1 are results of a model with snow storage. Discharge is generated from rain and melted snow in this model.

From qualitative comparison of the two simulated discharge curves in figure 4.2 it becomes clear that the equilibrium situation of the second model are almost or completely similar. Apparently, adding the snow storage causes little or no additional delay in generation of discharge from precipitation.

After examination of the temperature time series, it was found that temperatures are never below zero degrees Celsius in the Orinoco basin, not even on the highest places, according to this time series. Therefore no snow is formed in this model. In reality temperatures below zero degrees Celsius may occur, but due to the spatial resolution of the temperature data, these may have been averaged out.

4.4 Potential Evapotranspiration

It is assumed by the third model that not all water that enters the basin through precipitation leaves the basin through discharge, but that an amount of water is lost into the atmosphere through a potential evapotranspiration flux. In this model, evaporation is limited by the amount of precipitation and snowmelt. In reality, evapotranspiration is also limited by among others soil water availability, nutrient availability and diseases. Therefore the model evapotranspiration flux can be seen as potential evapotranspiration instead of actual evapotranspiration.

The following equation describes the water balance at location x, y at time step t.

$$R_{x,y,t} = P_{x,y,t} + PE_{x,y,t} + dS_{x,y,t}$$
$$S_{x,y,t} = SNS_{x,y,t}$$

R = runoff (mm)
P = precipitation (mm)
PE = potential evapotranspiration (mm)
dS = change in water volume stored (mm)
SNS = amount of water stored in the snow cover (mm)

Discharge is generated from runoff in a similar way as for the first model.

Potential evapotranspiration is calculated in two steps. In a first step, a potential evaporation from an extensive open water surface is determined by using the Thornthwaite equation:

$$E_{pot,Thornthwaite} = 16 * N_m \left(\frac{10\,\overline{T_m}}{I} \right)^a$$

$$I = \sum i_m = \sum \left(\frac{\overline{T_m}}{5} \right)^{1.5}$$

in which

$E_{pot,\ Thornthwaite}$ = potential evaporation from an extensive open water surface according to Thornthwaite
N_m = monthly adjustment factor related to hours of sunlight per day
T_m = monthly mean temperature in degrees Celsius
I = annual heat index
a = a cubic function of I
i_m = monthly heat index

In a second step this potential evaporation is converted to potential evapotranspiration of crops or land cover classes with crop coefficients. The crop coefficients are partly determined

by calibration. In the models of Kwadijk and Van Deursen it is assumed that potential evaporation from an extensive open water surface equals evapotranspiration of the reference crop that is standardly applied by the Food and Agricultural Organisation FAO. From most hydrological textbooks it can be derived that there's a clear distinction between potential evaporation and reference crop evapotranspiration (Ward and Robinson, 2000; Shuttleworth, 1993). From Doorenbos and Pruitt (Doorenbos and Pruitt, 1977) it can be derived that a potential evaporation can be converted to evapotranspiration of the standard reference crop by multiplying potential evaporation with 0,8 (Doorenbos and Pruitt, 1977). For this reason an extra conversion factor was added to the model that has been developed in this study. The modified second step now becomes:

$$ET_{pot,crop} = E_{pot,Thornthwaite} * cf * k_c$$

$ET_{pot,crop}$ = potential evapotranspiration of a crop or land cover class ($mm*t^{-1}$)
$E_{pot,Thornthwaite}$ = potential evaporation of an extensive open water surface according to the Thornthwaite equation ($mm*t^{-1}$)
cf = conversion factor potential evaporation to reference crop evaporation, 0,8
k_c = crop coefficient

Kwadijk and Van Deursen have calibrated evapotranspiration by introducing a reduction factor to the formula of the second step. The literature based crop coefficients were multiplied with this reduction factor to calibrate the amount of water that is lost by evapotranspiration.

The model was run until an equilibrium situation of the snow storage was reached on yearly basis. The equilibrium situation for each month in an average year on Puente Angostura is presented in figure 4.3, together with the equilibrium situation for the first two models.

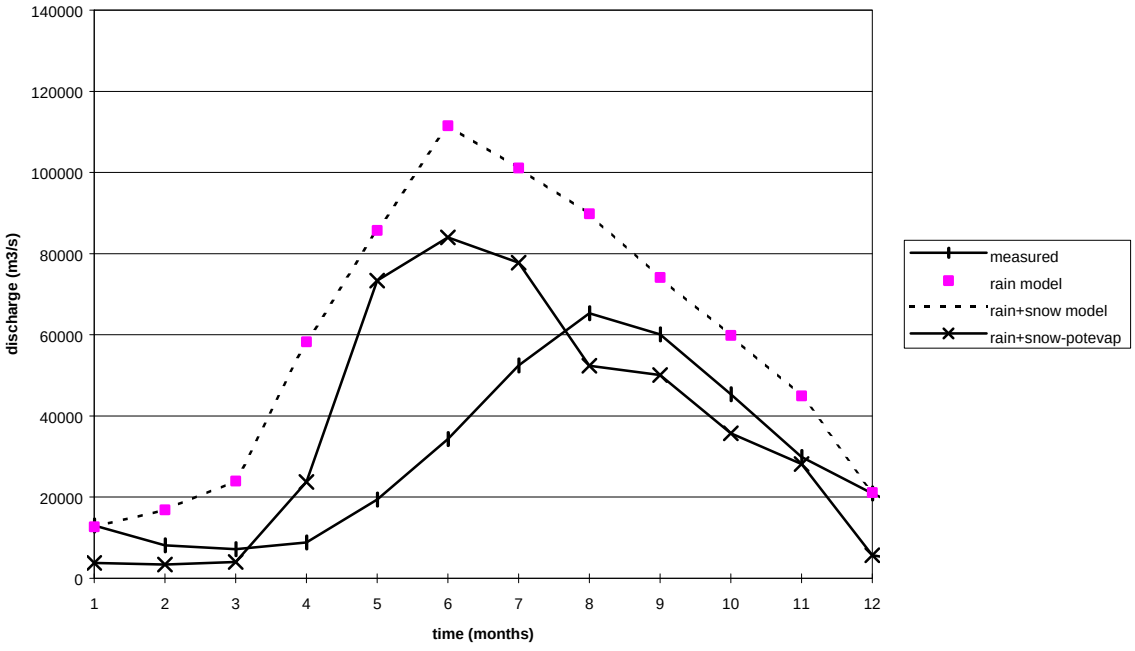

Figure 4.3 Monthly averaged measured and simulated discharge of three models.
Added in comparison with figure 4.2 are results of a model with potential evapotranspiration and snow storage. Discharge is generated from rain and melted snow minus potential evapotranspiration in this model.

From qualitative comparison of the three simulated discharge curves in figure 4.3 it becomes clear that adding the described equations to include potential evapotranspiration, results in lower discharge throughout the year. It can also be derived from figure 4.3 that the yearly discharge generated by the third model approaches the yearly measured discharge closer than the first two models.

4.5 Actual Evapotranspiration, linear

The fourth model is an extension of the third model with a soil water storage. Precipitation plus snowmelt minus evapotranspiration is added to this soil storage for each time step and runoff is only generated from this when the maximum water storage capacity of the soil is exceeded. Therefore the soil water storage causes a delay in the generation of runoff and discharge. The maximum water storage capacity of the soil is defined as the amount of water available in the soil for water suppletion of crops. This is approximately the amount of water stored in the soil between the soil water pressure at field capacity and the soil water pressure at wilting point. The amount of water stored in the soil is updated for each time step. Each time step the soil gains water from precipitation and snowmelt, and each time step the soil looses water due to evapotranspiration and runoff. Runoff occurs if the sum of the amount of water already stored in the soil and the inputs from precipitation and snow melt exceeds the maximum water storage capacity of the soil. The surplus of the soil water balance is used to calculate runoff.

Evapotranspiration is in this model not only limited by the sum of precipitation and snowmelt in a time step, but also by soil water availability. Evapotranspiration calculated by including limitation by soil water availability, is referred to as actual evapotranspiration in this study. Limitation of evapotranspiration by soil water availability can be modelled in several ways, of which two are discussed in this study: linear and exponential modelling. The fourth model includes linear limitation modelling. The linear way of modelling soil water limitation for evapotranspiration presumes that potential evapotranspiration takes place in a time step as long as it is smaller than the sum of water available in the soil storage plus precipitation and snowmelt that is added in that time step. When potential evapotranspiration is larger than this sum, then evapotranspiration is set equal to this sum. The following equation describes the water balance at location x, y at time step t.

$$R_{x,y,t} = P_{x,y,t} + AE_{x,y,t} + dS_{x,y,t}$$
$$S_{x,y,t} = SS_{x,y,t} + SNS_{x,y,t}$$

R = runoff (mm)
P = precipitation (mm)
AE = actual evapotranspiration (mm)
dS = change in water volume stored (mm)
SS = water stored in the soil (mm)
SNS = amount of water stored in the snow cover (mm)

Discharge is generated from runoff in a similar way as for the first model.

The model was run until an equilibrium situation was reached for the snow and soil water storages on yearly basis. The equilibrium situation for each month in an average year on

Puente Angostura is presented in figure 4.4, together with the equilibrium situation for the first three models.

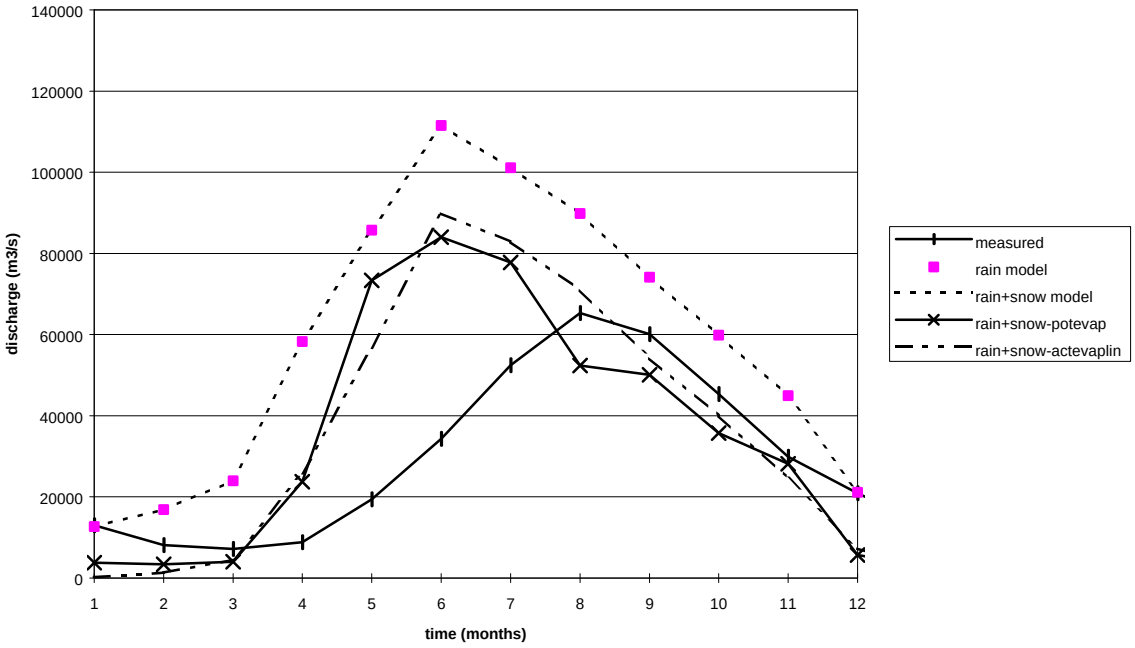

Figure 4.4 Monthly averaged measured and simulated discharge of four models.
Added in comparison with figure 4.3 are results of a model with actual evapotranspiration with linear function for soil water limitation, a soil storage and a snow storage. Discharge is generated from the excess of soil water after addition of effective precipitation.

From qualitative comparison of the four simulated discharge curves in figure 4.3 it becomes clear that the results obtained with the fourth model are not very much different from results obtained with the third model. The more or less smooth pattern in development of measured monthly averaged discharge throughout the year, is approached more by the fourth model than by the third model. The average amount of water coming to discharge on yearly basis is according to the fourth model not very much different than for the third model and therefore closer to the measured average yearly discharge than for the first two models.

4.6 Actual Evapotranspiration, exponential

The fifth model is different from the fourth model in the sense that limitation of evapotranspiration by soil water availability is modelled in an exponential way. When the added rain and snowmelt in a time step exceed potential evapotranspiration, evapotranspiration takes place at potential rate. In all other circumstances, evapotranspiration from the soil is not just assumed to be limited by soil water availability but also by aridity. The equations of Thornthwaite and Mather are used for this purpose. In this approach an estimate of the Accumulated Potential Water Loss APWL, which is an index for aridity, is made. For each time step i, APWL(i) is calculated as depending on the difference between precipitation and potential evapotranspiration and the initial soil water conditions. If the precipitation during time step i is sufficient to satisfy the demand of potential evapotranspiration, APWL(i) is set to 0, if the precipitation is less than potential evapotranspiration, APWL(i) is the sum of APWL(i-1) and the difference between potential evapotranspiration and precipitation. Actual evapotranspiration on time step i is a function of

the amount of moisture stored in the soil, the maximum water storage capacity of the soil and APWL(i).

Since this model is only different from the fourth model in the way that the evapotranspiration flux is modelled, and no new storages or fluxes were added, the water balance on a location x, y on a time t and generated discharge from runoff are similar to those of the fourth model.

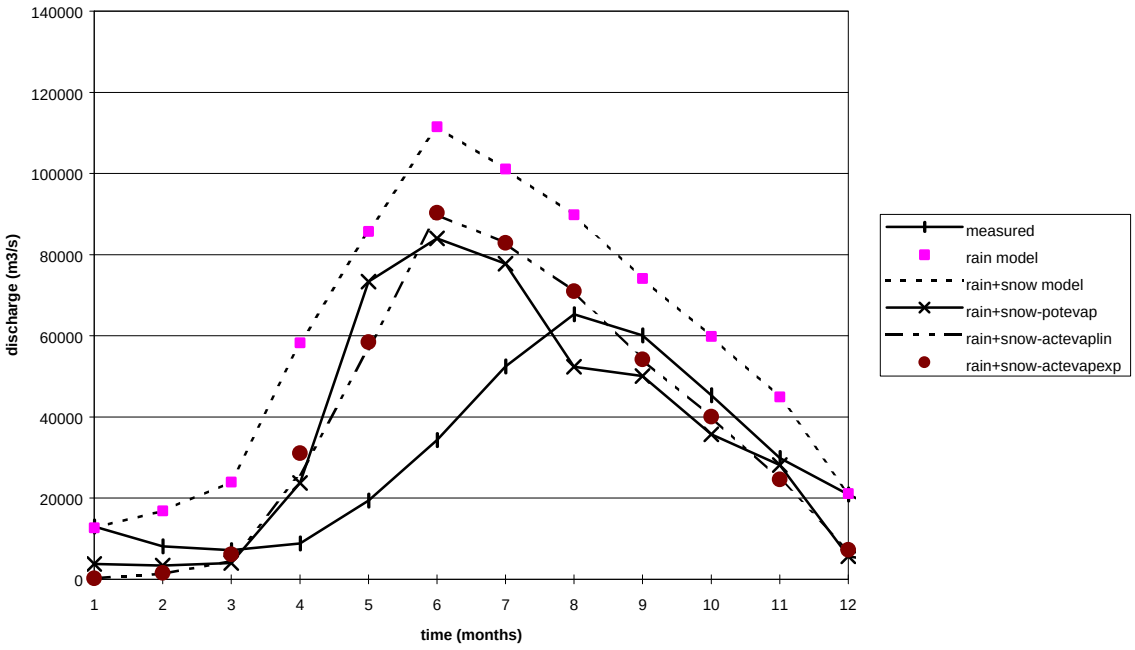

Figure 4.5 Monthly averaged measured and simulated discharge of five models.
Added in comparison with figure 4.4 are results of a model with actual evapotranspiration with exponential function for soil water limitation. a soil storage and a snow storage. Discharge is generated from the excess of soil water after addition of effective precipitation.

The model was run until an equilibrium situation was reached for the snow and soil water storages on yearly basis. The equilibrium situation for each month in an average year on Puente Angostura is presented in figure 4.5, together with the equilibrium situation for the first four models.

By qualitative comparison, results of generated monthly average discharge of the fifth model can hardly be distinguished from results generated by the fourth model. Differences in model results, originating from a different soil water limitation function for evapotranspiration appear to be small. Since the functions appear to be very different, it seems to be likely that limitation of evapotranspiration by soil water availability does not occur frequently on average.

4.7 Groundwater

The sixth model is an extension of the fifth model. Another storage is added to the model, representing deep groundwater and water stored in aquifers. To feed this storage, the runoff created on a location is separated into a part that comes to discharge rapidly, and a groundwater recharge part, that is added to the groundwater storage and comes to discharge with some delay.
The following equation describes the water balance at location x, y at time step t.

$$R_{x,y,t} = P_{x,y,t} + AE_{x,y,t} + dS_{x,y,t}$$
$$S_{x,y,t} = SS_{x,y,t} + GWS_{x,y,z} + SNS_{x,y,t}$$

R = runoff (mm)
P = precipitation (mm)
AE = actual evapotranspiration (mm)
dS = change in water volume stored (mm)
SS = water stored in the soil (mm)
GWS = water stored in the groundwater storage (mm)
SNS = amount of water stored in the snow cover (mm)

Discharge is generated from runoff in a similar way as for the first model.

In this model, the surplus of the soil water balance is separated into rapid runoff and groundwater recharge using a separation coefficient, which is calibrated.

$$sep = \frac{toGw}{Rapid\ Runoff}$$

sep = separation coefficient
toGw = groundwater recharge ($mm*t^{-1}$)
Rapid Runoff = the rapid runoff ($mm*t^{-1}$)

The groundwater recharge flux flows into the groundwater storage. From this storage delayed runoff representing the base flow of the river is calculated using a linear recession equation. The recession constant of this equation is calibrated.

$$Delayed\ Runoff = \frac{gwStor}{C}$$

Delayed Runoff = the delayed runoff ($mm*t^{-1}$)
gwStor = water in groundwater storage (mm)
C = a recession parameter (t)

The model was run until an equilibrium situation was reached for the snow, soil water and groundwater storages on yearly basis. The equilibrium situation for each month in an average year on Puente Angostura is presented in figure 4.6, together with the equilibrium situation for the first five models.

From qualitative comparison of the six simulated discharge curves in figure 4.6 it becomes clear that measured values of monthly average discharge are best approached by the sixth model and that this model makes a significant improvement on the other five models in describing averaged measured monthly discharge values.

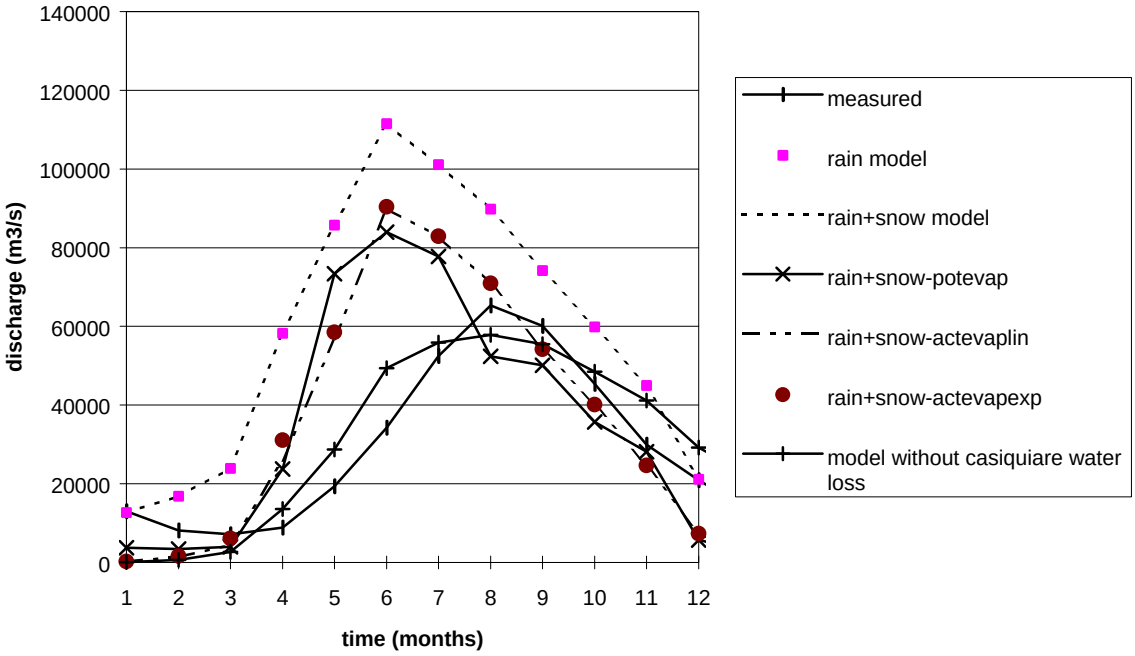

Figure 4.6 Monthly averaged measured and simulated discharge of six models.
Added in comparison with figure 4.5 are results of a model with actual evapotranspiration with exponential function for soil water limitation, a groundwater storage, a soil storage and a snow storage. Discharge is generated from two components. Rapid runoff is generated directly from a fraction of the excess of soil water after addition of effective precipitation. Delayed runoff is generated from emptying of the groundwater storage. Discharge is generated from the sum of delayed and rapid runoff.

4.8 Casiquiare diversion

In the seventh model, which is an extension on the sixth model, no fluxes and storages are added to the model. Therefore the water balance at a location is not influenced by this extension. In this model a factor is added that influences the generation of discharge from runoff. The peculiar transfer of water from the Orinoco basin to the Amazon basin through the Casiquiare channel (see chapter 2) causes less water to discharge in the Orinoco downstream of the Casiquiare channel – Orinoco fork than the amount that is generated as runoff upstream in the Orinoco basin. The seventh model takes this transfer of water into account by imposing a transport fraction limitation on the runoff routing and accumulation process at the fork location. On average, one third of the water is transferred towards the Amazon basin through the Casiquiare channel (WWF, personal communication). Therefore the imposed transport limitation fraction was set to the remaining share, two third.

The model was run until an equilibrium situation was reached for the included storages on yearly basis. The equilibrium situation for each month in an average year on Puente Angostura is presented in figure 4.7, together with the equilibrium situation for the first six models.

By qualitative interpretation of model results in figure 4.7 it can be found that results obtained with the seventh model closely resemble results obtained with the sixth model. Still, there is a clear distinction between results generated by the two models. As was to be expected, discharge values generated with the seventh model are somewhat lower than discharge values generated with the sixth model throughout the year.

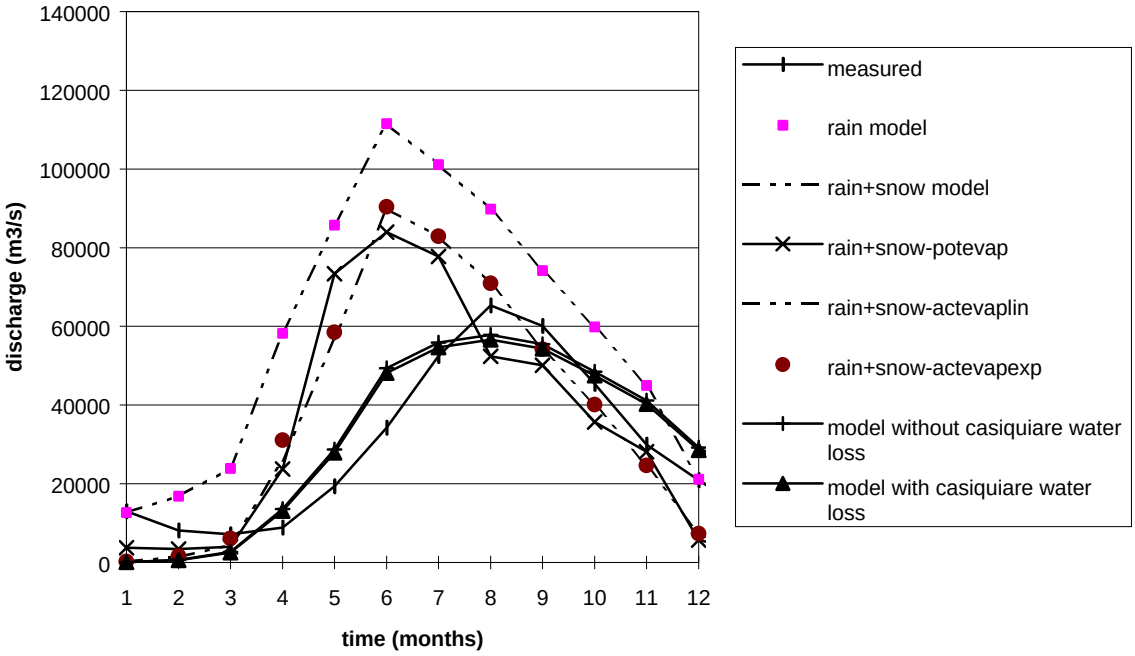

Figure 4.7 Monthly averaged measured and simulated discharge of seven models.
Added in comparison with figure 4.6 are results of a model with water losses from the basin through the Casiquiare channel, actual evapotranspiration with exponential function for soil water limitation. a groundwater storage, a soil storage and a snow storage. Discharge is generated from two components. Rapid runoff is generated directly from a fraction of the excess of soil water after addition of effective precipitation. Delayed runoff is generated from emptying of the groundwater storage. Discharge is generated from the sum of rapid runoff and delayed runoff. At the Casiquiare channel only a fraction of the discharge is allowed to pass.

4.9 Model Selection

From qualitative interpretation of model results, displayed in figure 4.7, it becomes clear that the sixth and the seventh model clearly distinguish themselves from the other five models. It can also be derived from figure 4.7 that not all processes contribute equally to the model performance. Since the first and second model produce the same results, the effect of the added snow storage on generated discharge at Puente Angostura is clearly insignificant. Furthermore, the difference between results of the fourth and fifth model seems to be very small. Adding a complex evaporation limitation function does not seem to offer much revenue, according to the models, for the average situation. The most significant improvements of performance of the average models seem to have been caused by adding an evaporation flux to the model and by adding a groundwater storage to the model.

The model with the highest performance, least complexity and most physical realism, is a model with soil and groundwater storages, water transfer to the Amazon basin and an evaporation flux with linear soil water availability limitation function seems to be the best choice. Still, the most complex model, which is the seventh model, was selected as model to base the Orinoco model on. Reasons for the fact that a snow storage and an exponential limitation function were included were the following. Although, the difference in performance between the exponential and the linear evapotranspiration limitation functions does not become clear from simulations with average models, it is expected that more significant differences do occur in simulations with actual data for dry periods. Since the Orinoco model should be able to simulate actual discharge, an exponential function was considered to be a

significant model improvement. Furthermore, although snow is an insignificant factor in the described average models, this may be caused by the resolution in temperature data (see paragraph 3.2), it may be a significant factor in reality. Therefore, it was chosen to keep the snow process in the model to allow for future snow simulations using improved temperature data.

The sixth and seventh model seem to perform much better in simulating measured monthly average discharge values at Puente Angostura than the other five. However, it must be taken into account that the choice of the best performing model was based on uncalibrated models with average input data and that performance was judged with average measured discharge. Theoretically it is not impossible that after calibration with actual data, one of the first five models appears to be much better able to describe measured discharge than the sixth and seventh model. When the worst performing average models are very sensitive to input data, dramatic changes in performance may occur in calibration with actual data. It was assumed that this was not the case.

5 Calibration and Verification

5.1 Calibration

Calibration is accomplished by finding a set of parameters that produce simulated discharges that match field measured discharge within a reasonable range of error. Measured discharge data was obtained from The Global Runoff Data Centre in Germany, the Ministerio del Ambiente y de los Recursos Naturales in Venezuela and the Instituto de hidrologia meteorologia y estudios ambientales in Colombia (appendix I). Field measured discharge, measured at Puente Angostura were used for calibration, since this measuring point is located near the Orinoco outlet and because a long time series of measured data was available for this point. Measured monthly discharge values of the period from 1965 to 1990 were used for calibration.

During previous studies a calibration procedure for the model concept has been developed (Kwadijk, 1993; Deursen, 1995). This calibration procedure was applied to calibrate the Orinoco model.

Two criteria are applied to calibrate the model:

1. Yearly simulated water discharge should correspond with yearly measured discharge assuming a stable model.
2. The timing and magnitude of peak and low flows, on a monthly time basis, should be well represented.

To meet the first criterion an average model can be applied. The model uses monthly input precipitation and temperature values averaged for the period between 1965 and 1990. In order to have a stable model, yearly change in storage of snow, groundwater and soil water should be equal to zero. This was realised by running the model until the storage contents showed no more changes on yearly basis. In the calibration procedure that was applied in previous studies, the equilibrium snow cover was compared with the measured snow cover. In situations where simulated equilibrium snow cover did not correspond with measured snow covered area, the snow melt rate model parameter was modified until a satisfying degree of correspondence was reached. Since there appeared to be no snow in the Orinoco basin, according to the developed model, calibration of the snow cover was not necessary here. The next step in the calibration procedure for the first criterion is to compare, the yearly simulated discharge of the stable model with yearly average measured discharge. When the simulated discharge did not correspond with measured discharge to a satisfying degree, evapotranspiration water losses were calibrated. This was done by modifying the reduction factor (see paragraph 4.4). A reduction factor of 1.55 resulted in a reasonable difference between simulated and measured average discharge of approximately 0.03 percent. A value of the reduction factor larger than 1 means that evapotranspiration is found larger than potential evapotranspiration. The most likely cause for this is poor performance of the Thornthwaithe formula within the occurring temperature window (Aerts et al, not reported). Theoretically, the error could also have been caused by incorrect values of maximum crop coefficients.

To meet the second criterion, the model was run with monthly input precipitation and temperature values averaged for the period between 1965 and 1990. In order to have timing and magnitude of the peaks and low discharge values correspond with measured values, a distinction was made between the rising and falling limb of the hydrograph.

The rising limbs of the discharge curves were calibrated by means of changing the separation coefficient (paragraph 4.7). This was done because for months with increasing discharge, the separation coefficient was expected to be of most influence on the shape of the hydrograph. Although physical backgrounds for variation of this coefficient can be found such as steepness, and soil physical properties, a single value of the separation coefficient has been applied for whole river basins in past studies by Kwadijk and Van Deursen.
The falling limb of the simulated hydrograph was calibrated by changing the recession coefficient (paragraph 4.7). This was done because for months with decreasing discharge it is assumed that discharge increasingly originates from slow runoff. The recession coefficient is mainly dependent on the geohydrological properties of a basin. Since no information about geohydrological properties of the Orinoco basin was available, one value for the recession coefficient was chosen for the whole basin.
The timing and magnitude of the measured peaks and low flows was reasonably represented by simulated values in a model with a separation coefficient of 0.25 and a recession parameter of 2. The results of this final calibration on discharge for station Puente Angostura is presented in figure 5.1.

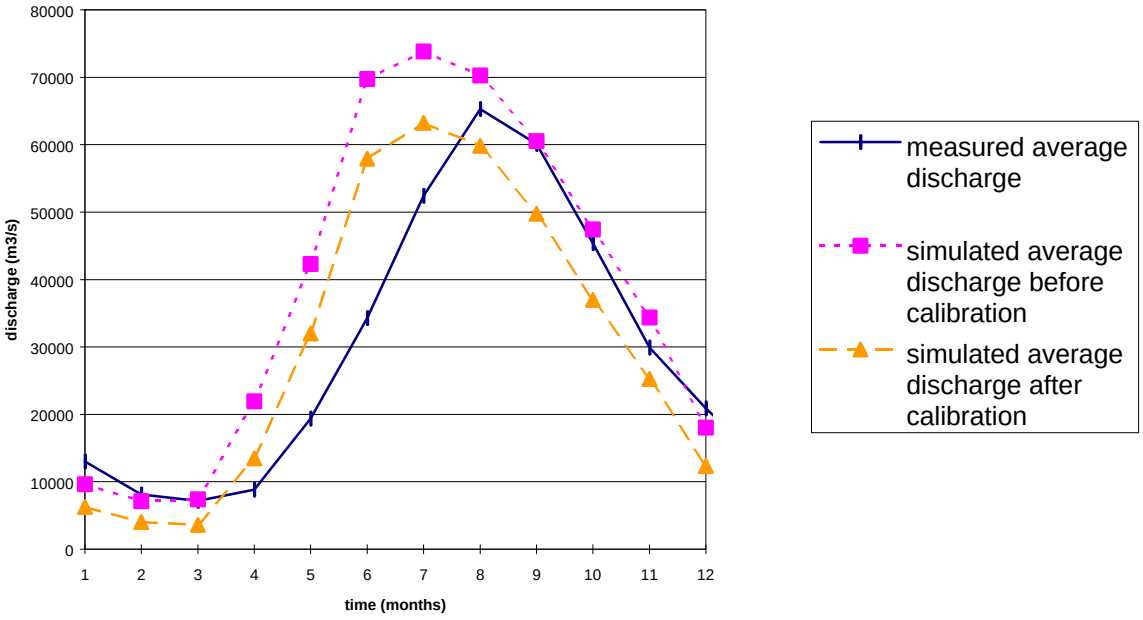

Figure 5.1 Monthly average simulated discharge before and after model calibration and monthly average measured discharge at Puente Angostura.

5.2 Evaluation of the calibration

In table 5.1 the results of calibration to meet the first criterion are presented. It becomes clear that the water balance has improved strongly due to calibration of the model. The yearly average simulated discharge approaches the yearly average measured discharge up to 0.03%.

Table 5.1 Yearly average measured discharge and simulated discharge before and after calibration.

yearly average discharge before calibration	1.2E+12 m^3
yearly average discharge after calibration	9.6E+11 m^3
yearly average discharge measured	9.6E+11 m^3

From figure 5.1 a qualitative impression can be formed to which extent the second criterion is met. By comparing timing and magnitude of peaks and low flows, an impression can be formed of the goodness of fit. It becomes clear that the calibration process improved model results in comparison with the uncalibrated situation. The general shape of the simulated discharge curve is similar to the general shape of the measured discharge curve. The timing of the month with lowest discharge according to the simulated and calibrated time series corresponds with that of the measured time series. However, the peak of the simulated and calibrated time series precedes the peak of the measured time series.

A common way of quantitatively evaluating calibration results is listing of measured and simulated discharge together with their differences and some type of average error in the calibration (table 5.2). In this study the average error between simulated and measured discharge was judged with the statistics mean absolute error and root mean square (RMS) error.

Table 5.2 Calibration results.
Measured and simulated average monthly discharge, their differences, mean absolute error and RMS-error.

month	measured average monthly discharge	simulated average monthly discharge	difference between simulated and measured
January	13030	6266	6764
February	8109	4035	4074
March	7153	3598	3555
April	8850	13461	4611
May	19393	32020	12628
June	34274	57927	23654
July	52437	63239	10803
August	65302	59835	5467
September	60115	49751	10364
October	45374	36972	8402
November	29911	25275	4636
December	20890	12349	8541
		Mean absolute error =	8225
		RMS-error =	10142

The mean absolute error and the RMS-error are both relatively large. This can partly be explained by the shift in time between simulated and measured discharge peaks. A small shift in time will already result in huge errors.

5.3 Verification

Model verification will help establish greater confidence in the calibration. A model is verified if its accuracy and predictive capability have been proven to lie within acceptable limits of error by tests independent of the calibration data.
Two verification steps were performed:

1. Verification at Puente Angostura, distinguishing between:
    - run 1 for the period 1965 – 1990 (not independent from calibration series);
    - run 2 for the period 1925 – 1965 (independent from calibration series).
2. Verification at other locations in the river basin

5.3.1 Verification at Puente Angostura

In a first step the developed model was verified at Puente Angostura by making use of other data than was used for calibration. Two verification runs were performed for this location.

- During verification run 1, time series of monthly precipitation and temperature of the time period between 1965 and 1990 were used to simulate monthly discharge on Puente Angostura. Since calibration was done with average model input data based on this data, the independence of this test can be argued. Therefore results should be interpreted carefully.
- During verification run 2, time series of independent monthly precipitation and temperature data for the time period between 1925 and 1965 were used.

Resulting simulated discharge in representative periods of 10 years are presented in figures 5.2 and 5.3 together with the measured discharge.

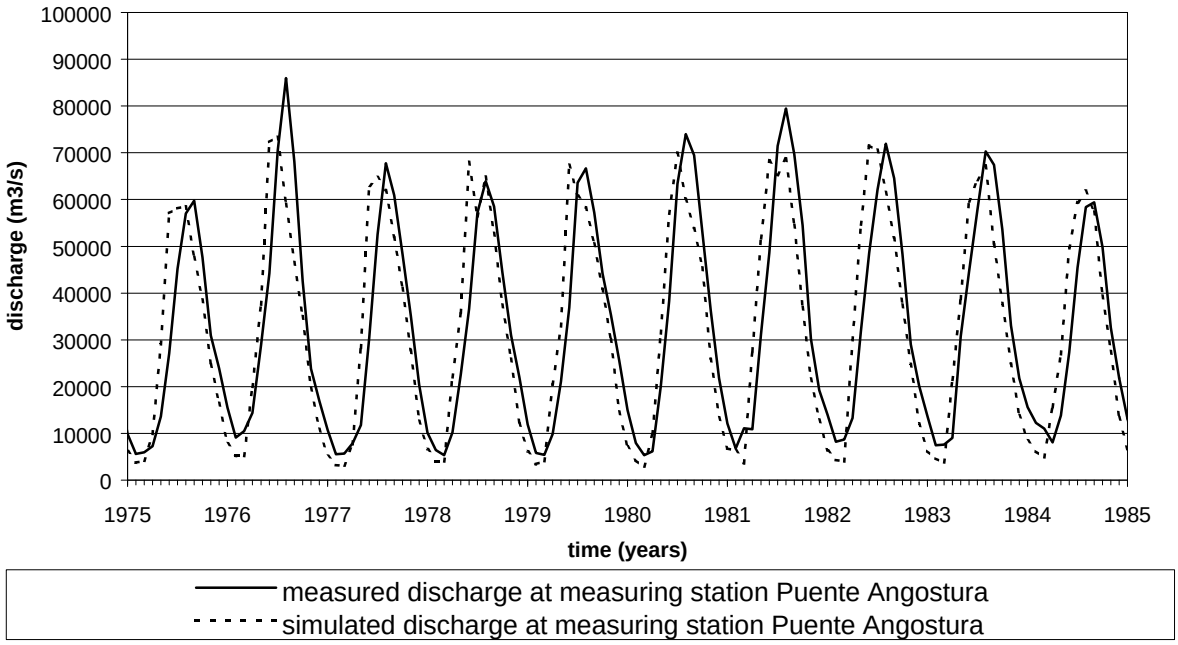

Figure 5.2 Simulated and measured discharge at Puente Angostura for verification run 1.

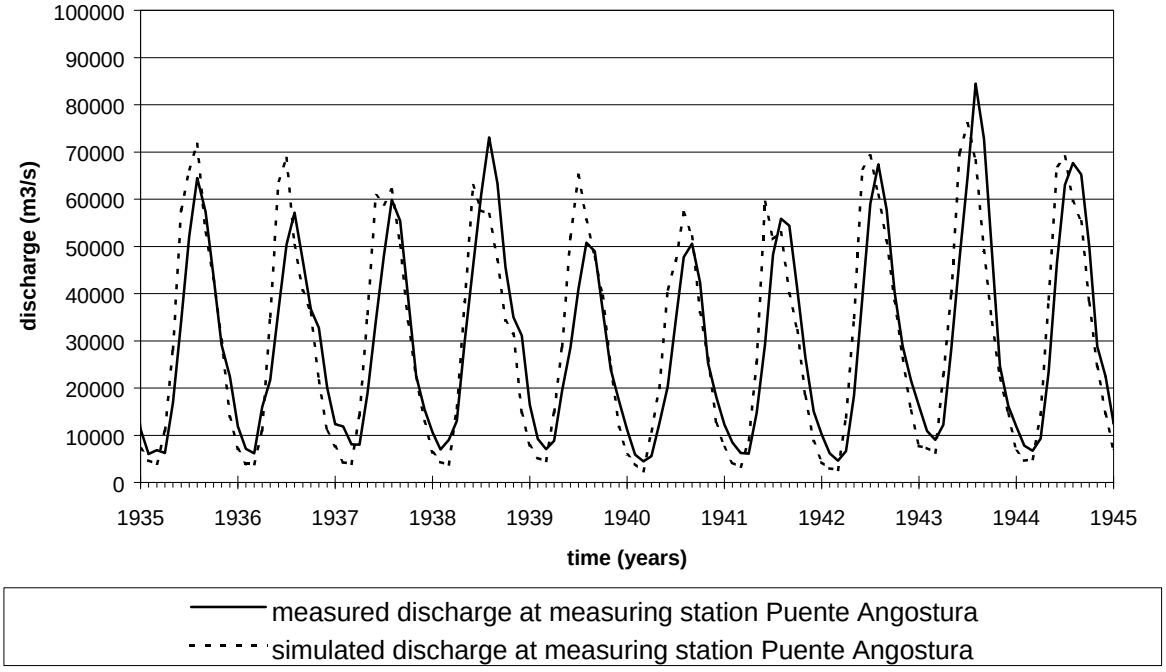

Figure 5.3 Simulated and measured discharge at Puente Angostura for verification run 2.

From qualitative interpretation of the verification results in figures 5.2 and 5.3 and comparison with the calibration results (figure 5.1), it becomes clear that the results of the verification runs show the same patterns as the results of the calibration run. Timing of the month of lowest discharge is quite well represented by both results, but simulated peak values are shifted in time. During quantitative interpretation of results of the verification runs, mean absolute errors and RMS-errors were determined. Furthermore the errors in the total amounts of water coming to discharge during the simulated periods were determined. These errors are presented in table 5.3, together with calibration results.

Table 5.3 Mean absolute errors and RMS-errors in calibration and verification series at station Puente Angostura.

RMS-error 1925-1965 verification series	11596 m^3/s
RMS-error 1965-1990 verification series	12183 m^3/s
RMS-error calibration series	10142 m^3/s
Mean absolute error 1925-1965 verification series	8868 m^3/s
Mean absolute error 1965-1990 verification series	9734 m^3/s
Mean absolute error calibration series	8225 m^3/s
Error in total discharge 1925-1965 verification series	3.98%
Error in total discharge 1965-1990 verification series	0.23%
Error in total discharge calibration series	0.03%

Table 5.3 shows that RMS and mean absolute errors in verification results are of the same order of magnitude as the errors determined from the calibration result. As was explained before, the magnitude can partly be explained by the fact that simulated peaks are somewhat shifted in time. The error in total discharge for the periods between 1925-1965 and 1965-1990 are significantly larger than the error obtained during calibration. Still, these errors are considered to be within reasonable limits. Results of verification run 1 are interpreted as positively contributing to confidence in model performance.

5.3.2 Verification at other locations

A second step in the verification procedure was to determine if the model was able to reliably simulate discharge values at locations in the basin other than the calibration station of Puente Angostura. For this step it was only possible to use model input data which were also used for calibration. This was the only option since measured data at other hydrographic measuring stations were available only for after 1965. The data series used for verification are therefore not completely independent. This should be taken into consideration during interpretation of results. Two verification runs were made, one with averaged input data and one with non-averaged input data

- During verification run 1 simulations were made with average monthly precipitation and temperature from 1965 to 1990 and results were compared with average monthly discharge based on part of this period. Resulting simulated monthly average discharge for measuring stations Aceitico in the Meta River and Santa Rita in the Vichada River are presented in figure 5.4 a and c, together with measured values.
- During verification run 2 simulations were also made with non-averaged data. Time series of monthly precipitation and temperature from 1965 to 1990 were used for these simulations. Results of these simulations for measuring stations Aceitico and Santa Rita are shown in figure 5.4 b and d, together with measured values.

Results obtained for measuring stations Musinacio, San Fernando, Puente International, Pie de Salto, Roncador, Puente Narino, Guayare and Tama Tama are presented in appendix II.

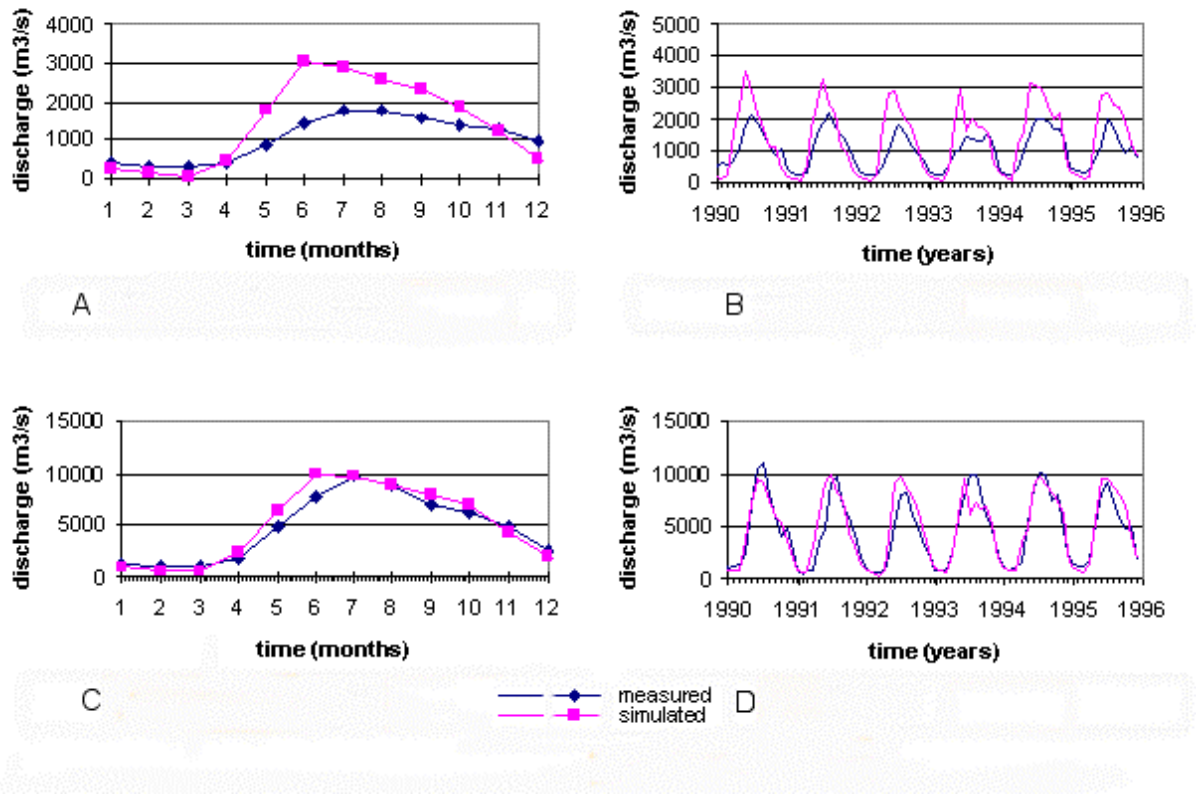

Figure 5.4 a-d Simulated and measured discharge used for verification.
A monthly averaged discharge at station Sta. Rita
B monthly discharge at station Sta. Rita
C monthly averaged discharge at station Aceitico
D monthly discharge at station Aceitico

From qualitative interpretation of figure 5.4 and the results presented in appendix II it is concluded that the ability of the model to simulate discharge at other measuring stations than

Puente Angostura was quite poor for most stations. Results for station Aceitico (fig. 5.4), near the inflow point of Meta tributary and station Roncador, in the Orinoco main stream just upstream of Meta tributary were positive exceptions to this.
Absolute mean errors and RMS-errors for discharge simulations at other stations than Puente Angostura are presented in table 5.4.

Table 5.4 Mean absolute errors, RMS-errors and relative RMS-errors of the average model and the model with time series of data, for the stations that are shown in figure 2.4.

station	Average model			Time series model			
	Absolute mean error	RMS-error	relative RMS-error	Absolute mean error	RMS-error	relative RMS-error	observed values - n
Orinoco – Puente Angostura	8625	10142	33.36	9735	12183	39.14	300
Apure – San Fernando	773	1013	65.22	506	661	42.54	36
Orinoco - Musinacio	11607	13885	48.32	8873	10743	37.38	36
Arauca – Pte International	256	362	94.72	269	355	92.86	36
Caura – Pie de Salto	658	715	29.01	574	765	33.44	129
Meta - Aceitico	689	910	19.11	983	1354	28.66	155
Orinoco - Roncador	3032	3859	25.37	3869	5494	36.30	156
Vichada – Sta Rita	572	739	71.12	560	739	72.46	72
Orinoco - Puente Narino	3641	4043	27.74	4474	5649	37.84	128
Guaviare - Guayare	1600	1956	28.41	1949	2499	36.00	106
Orinoco – Tama Tama	1329	1582	128.96	1385	1716	139.86	132

Table 5.4 confirms some of the observations that were made during qualitative interpretation of the results of the second verification step. The relative RMS-errors are relatively low for stations Aceitico and Roncador. Relative RMS-errors for these stations and stations Puente Narino and Guayare are lower than relative RMS-errors at the calibration point, Puente Angostura. This could be interpreted as the model performing better at these stations than at the calibration point. However, results at Puente Narino and Guayare (appendix II) show significantly larger relative differences between measured and simulated peaks and low values than Puente Angostura (figures 5.2, 5.3). This is likely to be caused by the fact that simulated peaks of these stations are less shifted in time than the peaks of Puente Angostura.
The model has clearly not shown to be valid within the simulated timeframe for the areas upstream of stations Puente International in the Arauca tributary, Santa Rita in the Vichada and Tama Tama in the Orinoco main stream. Poor model results for station Tama Tama are partly caused by imperfections in the stream network near this station.

An impression of the spatial distribution of simulated discharge can be obtained from figures 5.5 and 5.6.

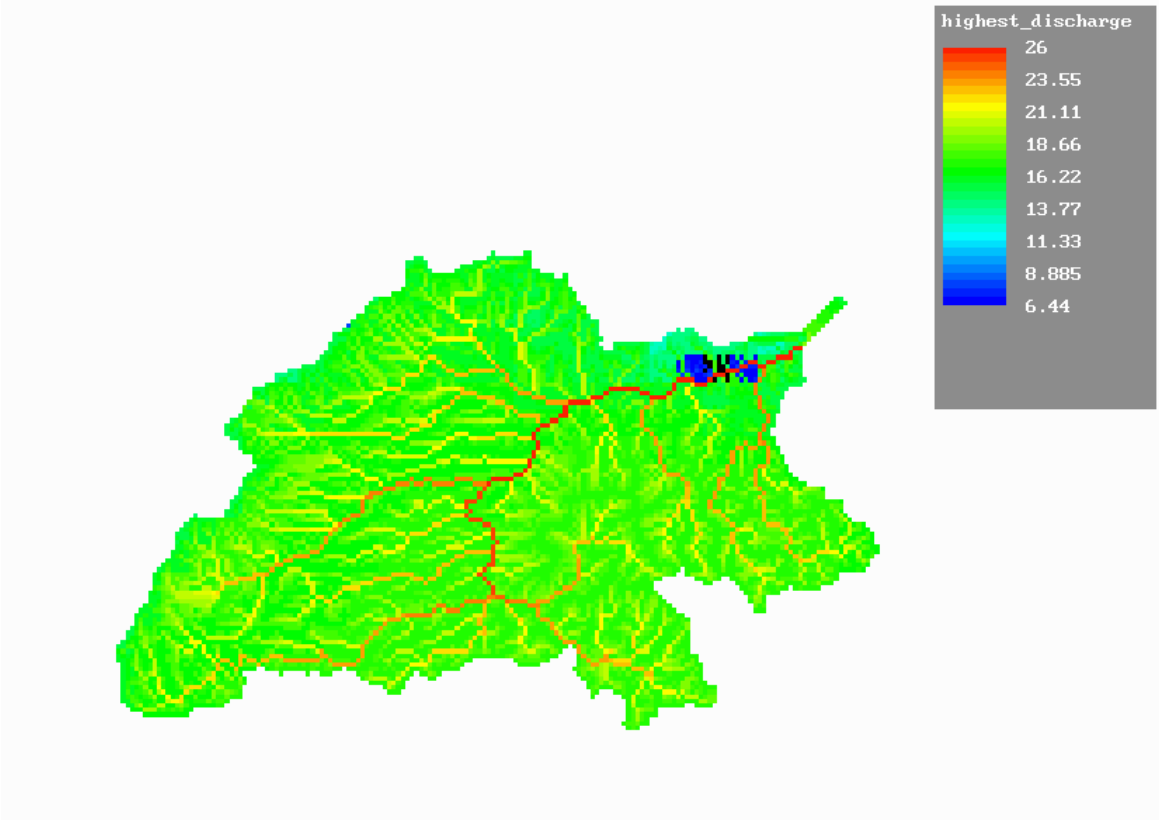

Figure 5.5 Simulated discharge (m3/s) in the Orinoco basin during the month with highest simulated discharge (July), logarithmic values.
Black cells represent areas with zero discharge due to missing input data.

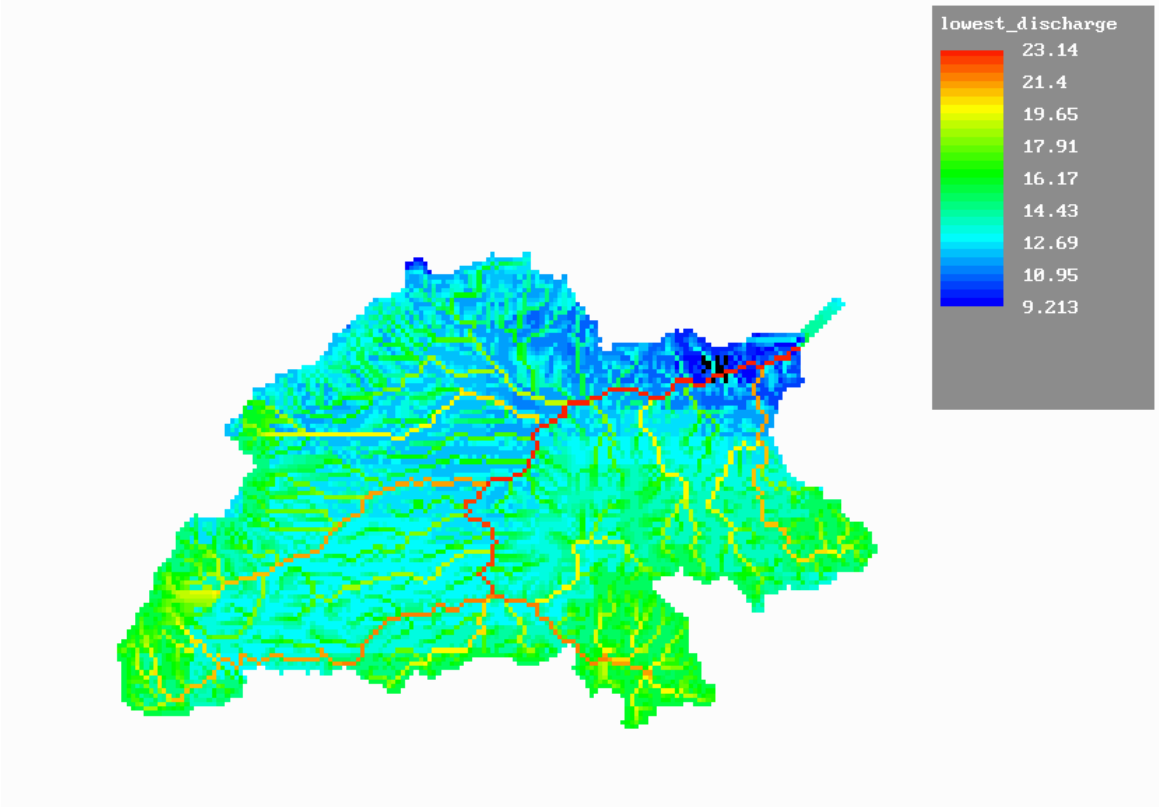

Figure 5.6 Simulated discharge (m3/s) in the Orinoco basin during the month with lowest simulated discharge (March), logarithmic values.
Black cells represent areas with zero discharge due to missing input data.

5.4 Evaluation

From the results of calibration and verification it can be concluded that the model is reasonably well able to simulate monthly averaged discharge at station Puente Angostura between 1923 and 1990 and non-averaged monthly discharge based on this timeframe, but that peaks are shifted in time one to three months. Verification results for this measuring point are of a more or less similar quality as calibration results. Verification results for station Aceitico, at the inflow of the Meta River and Roncador in the Orinoco main stream were better than calibration and verification results on Puente Angostura, by qualitative and quantitative interpretation of results. As the used verification data series for these stations were not totally independent from calibration data series, the validity of the model for these stations will have to be proved by simulations with totally independent verification data series.
As yet it has not been shown that the model is valid for simulating discharge in the upper regions of Arauca tributary and the Orinoco main stream, as well as the Vichada river.

A major model assumption is that all runoff reaches the outflow point of the Orinoco within one time step. Upstream stations reflect discharge of smaller sub catchments with smaller maximum travel time of runoff from the catchment boundary to the measuring station. Therefore a relatively small time step would be appropriate at these stations. For measuring stations that are located more downstream, maximum travelling time of runoff from the catchment boundary may be large. A larger time step would be appropriate for these stations. When this maximum travelling time exceeds the model time step, the assumption that all runoff reaches the outflow point of the Orinoco within one time step is not completely valid. As was already illustrated by some simple calculations in paragraph 3.1, this could be the situation for some measuring stations that are located downstream in the catchment of the Orinoco River. Such a situation would be reflected in a shift in time of simulated discharge curves with respect to measured discharge. The shift in time that is visible in the simulated discharge peaks and low values on Puente Angostura with respect to measured values could be caused by the choice of the time step of one month, as this measuring station is located far downstream of the catchment boundary. This hypothesis is supported by the observation that the shift in peaks and low values is not visible in discharge for stations located high upstream in the river basin (e.g. Pie de Salto, Guayare, see appendix II) and that it is visible for another station than Puente Angostura, located relatively downstream in the river basin, Musinacio station (see appendix II). During further studies with other time steps than one month the validity of the hypothesis may be tested.

6 Limitations and Scenarios

6.1 Limitations

A distinction between two types of model limitations was made: limitations due to the spatial and temporal resolution of the model and limitations due to calibration and verification.

6.1.1 Limitations due to spatial and temporal resolution

The input map with the lowest resolution had a resolution of 0.5*0.5 degrees. No statements can be made on a scale smaller than this, since the spatial distribution within a 0.5 degree grid is not known (approximately 60*60 km).

Calculations of slope gradient and exposition for drainage delineation from a DEM with a 3*3 km resolution do not have any physical meaning. Therefore, an accurate estimation of local overland flow direction is not possible with this modelling concept. Using this resolution there is no physical background to separate horizontal water flow into direct and delayed runoff. Hence, flows such as Hortonian overland flow and saturated overland flow are not incorporated into the model. The separation of the different flow types may only be possible on small scale plots (e.g. Ward and Robinson, 2000). The model has been developed to analyse the discharge of the River Orinoco and the major tributaries on a monthly time basis. Using this time basis and a basin scale the contribution of different flows (saturated and Hortonian overland flow, interflow and groundwater flow) to the stream flow may not be relevant. For the River Orinoco, therefore, runoff is proportionally separated into quick and delayed runoff.

Since the width of river channels in the Orinoco basin is usually less than 10 km, the drainage analysis does not make any statements about the nature (braided, meandering or anastomosing) of the channels. Cells located in the river sections do not imply that the river is actually 10 km wide, but the location of a cell in a river section means only that there is a flow path through that cell. The model concept assumes that all water available for stream flow in the large tributaries will leave the basin within one time interval. Therefore the model has not been developed to incorporate any in-channel processes, such as hydraulic routing. Consequently, the nature of the channels is not relevant.

6.1.2 Limitations due to calibration and verification

The model was calibrated for the time period between 1965 and 1990 on station Puente Angostura. Verification was done for this station for the time period between 1923 and 1965. Model results for station Puente Angostura were reasonably well for both calibration and verification. Model results for other stations in the basin were in some cases good and in some cases not so good, but in all cases insufficiently verified. The model may therefore only be used for simulation of discharge at Puente Angostura measuring station.

The model uses empirical equations, which have been developed and tested for conditions from 1923 until 1990. It is clear that, if these equations are not valid under other conditions, the results will be less reliable. Therefore results of simulations beyond the range that the model was tested for must be handled with care.

6.2 Scenarios

6.2.1 Interventions

To illustrate the usefulness of the model for simulation of the effects of human interventions on river discharge, two examples of hypothetical scenarios are presented in this chapter. The first scenario involves construction of a dam. The second scenario pertains to water diversion from the Guaviare River to the Amazon basin. In reality, these two interventions mainly influence the division of surface water in the river basin in time and in space. In the model, the interventions influence generation of discharge from accumulation of runoff through routing (paragraph 3.2.2). These interventions do not influence the water balance that is calculated within each cell, since water produced on one location is assumed not to contribute to the water balance of other locations. According to the model limitations described in the previous paragraph, the model is assumed to be only valid under the circumstances that effects of interventions fall within the range of conditions present in calibration and verification series. The changes in discharge due to both interventions are expected to fall largely within that range. Therefore the model is assumed to be valid under the circumstances that the interventions have taken effect. Since the model is only considered to be valid for simulating discharge at measuring station Puente Angostura, effects of the interventions on discharge at this measuring point can be studied.

6.2.2 Example 1: Construction of a dam

Vonk (2001) developed a script for the simulation of dams and reservoirs in PCRaster. This script is used in this example to simulate a hypothetical dam located in the Ventuari River (figure 6.1).

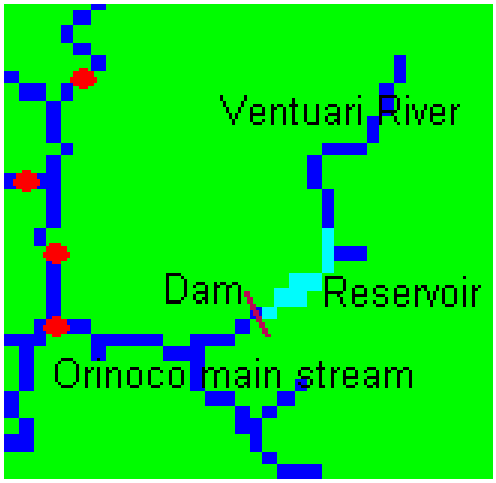

Figure 6.1 Estimated reservoir area of a dam with hypothetical characteristics in the Ventuari River.

The hypothetical dam was assumed to be used for generation of electricity at a constant level, and has been given a height of 158m, which was estimated with scripts developed by Vonk (2001). The design power of the dam was estimated to be approximately 2500 MW.

Simulations were made with input climatic data from the period 1965-1995.
The calculated hypothetical reservoir area of the hypothetical dam is shown in figure 6.1. Although estimates were made of dam and reservoir characteristics to obtain realistic values, it should be considered that accuracy in these estimates is quite low. The accuracy of the estimates is to a large extent determined by the representation of the dam and reservoir on the digital elevation model. The higher the amount of raster cells that cover the real dam and

reservoir, the more accurate are the estimates of dam characteristics. In the used digital elevation model, the raster cell size is 10*10 km. Therefore the minimum length of a dam is 10 km. In reality, length and width of dams are usually much less than 10 km. However, the characteristics that are used for the dam functioning (active volume and firm discharge) were not directly dependent on the resolution of the digital elevation model. Therefore the low resolution of the digital elevation model is expected not to influence calculated discharge directly.

Discharge at measuring station Puente Angostura before and after construction of this hypothetical dam are presented in figure 6.2. Measuring station Puente Angostura is located far downstream of the hypothetical dam (figure 2.4).

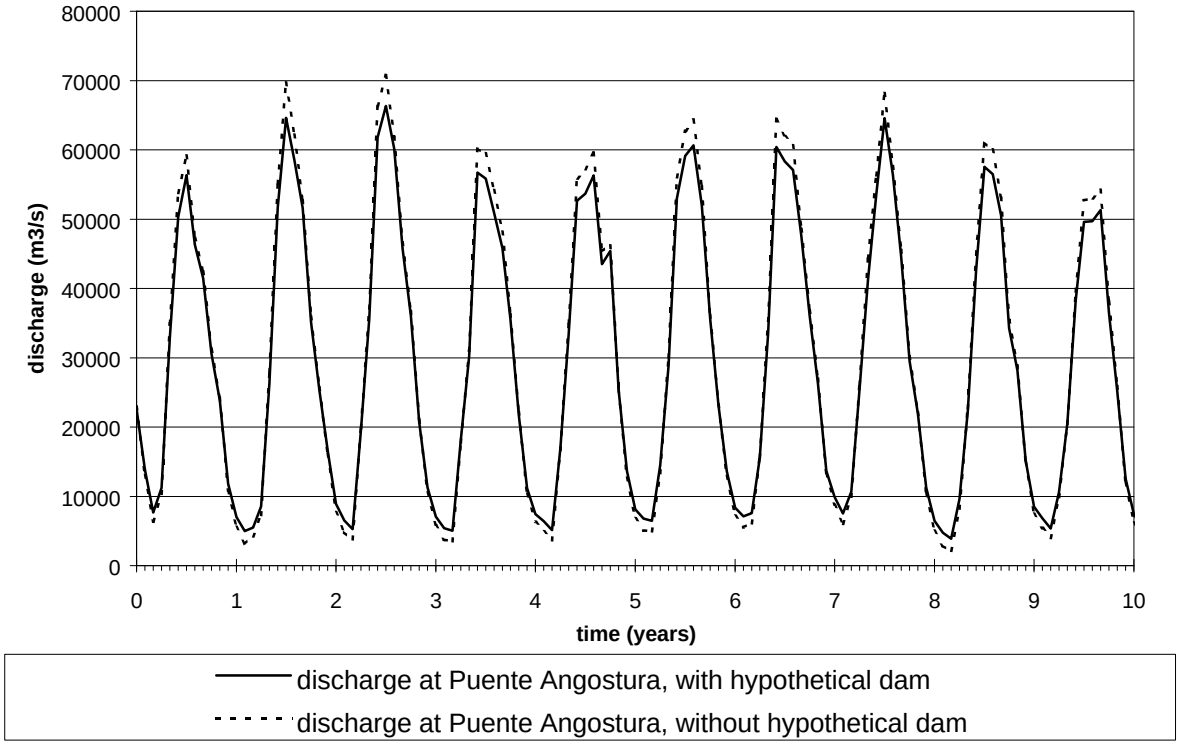

Figure 6.2 Effect of dam on basin scale. Simulated discharge at Puente Angostura for the situations with and without a hypothetical dam in the Ventuari River, with hypothetical dam characteristics.

From figure 6.2 it becomes clear that the dam causes a decrease in the amplitudes of the hydrograph. Although the absolute decrease is quite large during a part of the simulated period, the decrease relatively is small with respect to total discharge.

The effect of the hypothetical dam and reservoir in the Ventuari River on discharge at Puente Angostura was quantified. Since the calculations were based on hypothetical data, quantification only shows expected changes under the specified conditions. A distinction was made between effects of the dam and reservoir on discharge during the season with high discharge and the season with low discharge. These seasons were for every year determined on the basis of long term average simulated discharge in the situation without a dam and reservoir. Results are presented in table 6.1

Table 6.1 Effects of a dam in the Ventuari River on discharge at measuring station Puente Angostura, far downstream of the dam, during the high and low discharge periods of the year.

effect on basin discharge	high discharge season	low discharge season
mean total discharge ($m^3 * 10^6$), no dam	761604	212230
mean total discharge ($m^3 * 10^6$), with dam	725351	223756
difference in total discharge due to dam ($m^3 * 10^6$)	-36254	11526
percentual difference in discharge due to dam (%)	-4.8	5.4

Local effects of the diversion are shown in figure 6.3. The effect of the diversion on discharge at a location in the Ventuari River, downstream of the dam, just before the Ventuari River dissipates into the Orinoco River is shown.

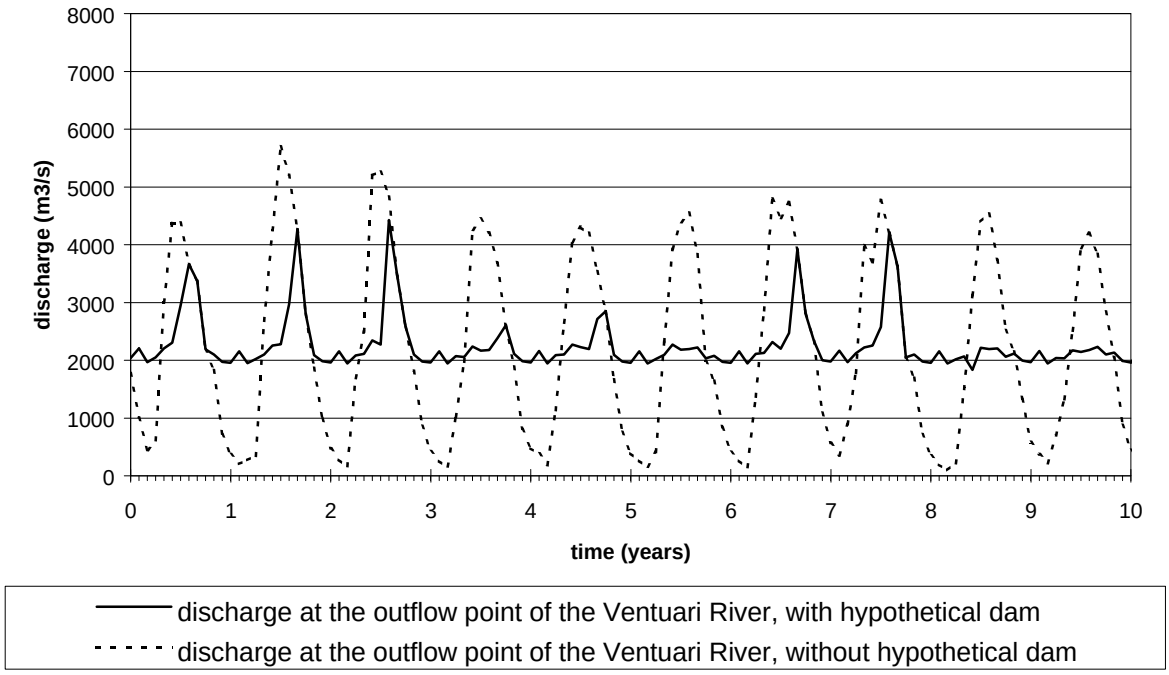

Figure 6.3 Local effect of dam. Simulated discharge in the Ventuari River near the point where it dissipates into the Orinoco main stream.

Figure 6.3 shows that the effect of a hypothetical dam in Ventuari River on discharge just downstream of the dam is quite large. Because of the constant normal throughflow of the dam, the simulated discharge pattern just downstream of the dam is quite constant most of the year. Often, in the high discharge season, a part of the reservoir volume is released through the emergency spillway, which results in high peaks of discharge downstream of the dam during these periods.

The effect of the dam and reservoir on river discharge at the location in Ventuari River downstream of the dam and reservoir was quantified. Results of this quantification are shown in table 6.2.

Table 6.2 Effects of a dam in the Ventuari River on discharge in the Ventuari River, near where it dissipates into the Orinoco main stream.

local effects	high discharge season	low discharge season
mean total discharge ($m^3 * 10^6$), no dam	65081	18822
mean total discharge ($m^3 * 10^6$), with dam	45868	37710
difference in total discharge due to dam ($m^3 * 10^6$)	-19213	18888
percentual difference in discharge due to dam (%)	-29.5	100.3

Table 6.2 shows an enormous increase of discharge in the Ventuari River, downstream of the dam, during the low discharge season due to the dam and reservoir and a significant decrease in discharge during the high discharge season.
From the results of the scenario that was described in this paragraph it can be concluded that although effects of a dam and reservoir high upstream in the river basin may be relatively small on basin scale, local effects can be large.

6.2.3 Example 2: Diversion of a part of the water towards another river basin

The second intervention of which consequences on discharge were explored was a diversion of a part of the water of the Guaviare River through a channel towards the Rio Negro in the neighbouring Amazon basin. A main purpose of this diversion is to be able to transport goods from eastern Colombia to Brazil over inland waterways (personal communication, WWF). A hypothetical location for the point where water could be abstracted from the Guaviare River was determined with a detailed map with water courses. A point where the Guaviare River and Rio Negro come close and where Rio Negro seems already large enough for navigation according to the upstream area was chosen as starting point of a hypothetical channel. In the model this channel was implemented in such a way that only a fraction of the discharge entering the cell on which the channel starts in the Guaviare River is let through to reach the outflow point of the Orinoco. On the splitting point, one third of the discharge was assumed to proceed through the Guaviare River and this amount is let through. The remaining two third of the water is assumed to be transferred from the start of the diversion out of the basin. Simulations were made with input climatic data from the period 1965-1995.

The fraction of water flowing in either direction at the splitting point will most probably vary throughout the year, depending on regulation, the amount of discharge and streambed profiles in reality. Since no information is available on these subjects, the fractional division of water was assumed in the model.

Figure 6.4 shows the location of the start of the diversion, together with simulated discharge in the diversion scenario. A decrease in discharge is visible in the Guaviare River in the area directly downstream of the diversion point with respect to the area directly upstream of the diversion point.

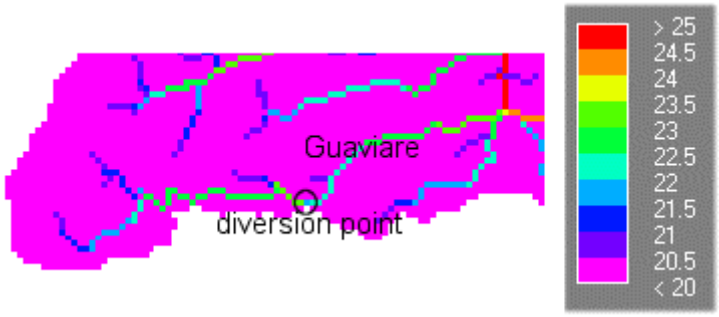

Figure 6.4 Effects of a diversion on discharge (m^3/s) of the Guaviare River, logarithmic values.

Results of the diversion channel on discharge at Puente Angostura, which is located far downstream of the diversion, are presented in figure 6.5.

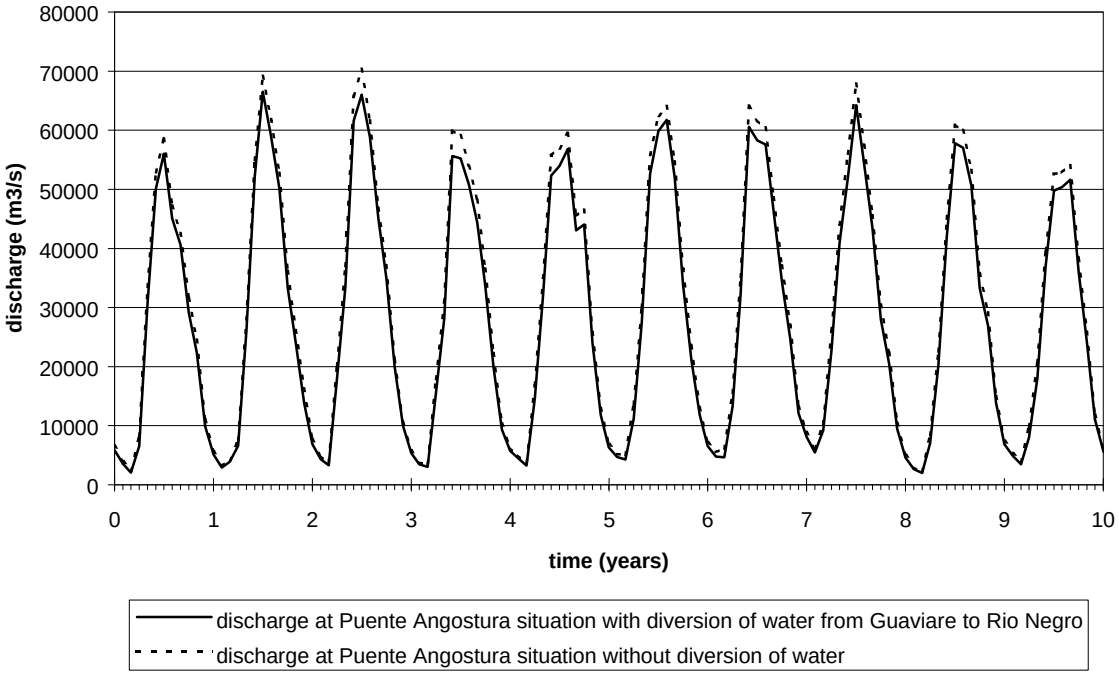

Figure 6.5 Effects of diversion on basin scale. Simulated discharge at Puente Angostura for the situation with and without a diversion of water from the Guaviare River to the Rio Negro.

Figure 6.5 shows a decrease of peaks and low values of discharge at Puente Angostura, resulting from diversion of water from the Guaviare River to the Rio Negro. From this figure it seems that effects of the diversion on discharge at Puente Angostura are relatively small.

The effect of the diversion of water to Rio Negro on the discharge at Puente Angostura was quantified. Since the calculations were based on hypothetical data, quantification only shows expected changes under the specified conditions. A distinction was made between effects of the diversion on discharge during the season with high discharge and the season with low discharge. These seasons were for every year determined on the basis of long term average simulated discharge in the situation without a diversion. Results are presented in table 6.3

Table 6.2 Effects of a diversion on discharge at measuring station Puente Angostura, far downstream of the diversion, during the high and low discharge periods of the year.

Effects on basin discharge	high discharge season	low discharge season
mean total discharge ($m^3 * 10^6$), no diversion	762916	208447
mean total discharge ($m^3 * 10^6$), with diversion	722395	187823
decrease in total discharge due to diversion ($m^3 * 10^6$)	40513	20625
percentual decrease in discharge due to diversion (%)	5.3	9.9

Table 6.3 confirms that although the decrease in discharge at Puente Angostura due to the diversion amounts several thousands of cubic meters during parts of the simulated period, the decrease is relatively small.

Local effects of the diversion are shown in figure 6.6. The effect of the diversion in discharge at measuring station Guayare is shown.

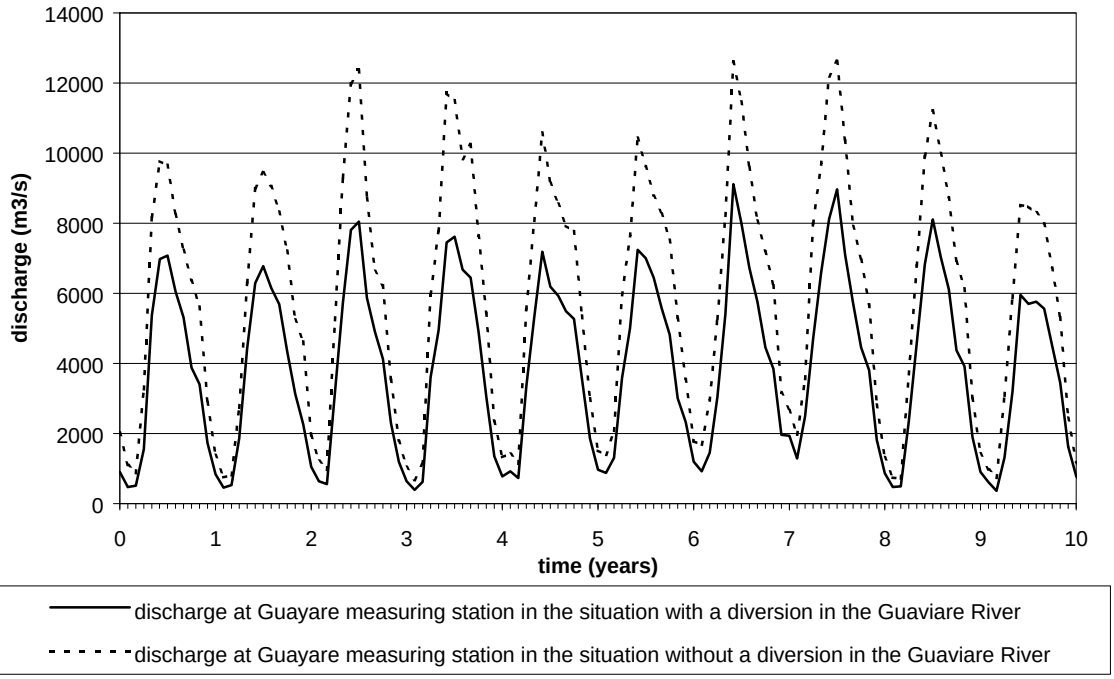

Figure 6.6 Local effects of diversion. Simulated discharge at Guayare measuring station for the situation with and without a diversion of water from Guaviare River to the Rio Negro.

Figure 6.6 shows a significant decrease in simulated discharge at Guayare measuring station due to the diversion of water from the Guaviare River towards the Rio Negro.

The effect of the diversion on discharge at Guayare measuring station was quantified. Results of the quantification are shown in table 6.4.

Table 6.3 Effects of a diversion on discharge at measuring station Guayare, near the diversion point, during the high and low discharge periods of the year

local effects	high discharge season	low discharge season
mean total discharge ($m^3 * 10^6$), no diversion	148536	33387
mean total discharge ($m^3 * 10^6$), with diversion	100775	19941
decrease in total discharge due to diversion ($m^3 * 10^6$)	47761	13446
percentual decrease in discharge due to diversion (%)	32.2	40.3

Table 6.4 shows that effects of the diversion on discharge at Guayare measuring station are large, both in absolute and relative sense.

From the results of the scenario that was described in this paragraph it can be concluded that although effects of a diversion high upstream in the river basin may be relatively small on basin scale, local effects can be large.

7 Evaluation and recommendations

7.1 Evaluation

The hydrological cycle of a river basin may be viewed as a series of storages and flows. A water balance is often used as a framework to describe the transformation of input (precipitation) through this cycle. The algorithms to describe the different flows through the compartments may differ from completely empirical to more conceptual. In a conceptual model, more consideration is given to the physical processes acting on the input variables to produce the outflow. A disadvantage of conceptual models is that they usually require large amounts of input data.
The availability of data and the time available for model construction determined the ultimate selection of a suitable model type to simulate discharge in the Orinoco basin. As the time available for model construction was relatively small, a distributed water balance approach was selected for the surface water model. As there was little time to collect detailed data from databases in Venezuela and Colombia, most data have been derived from readily available databases on the internet. The model developed must be seen in the light of these two main constraints.

The developed model is able to simulate monthly discharge at hydrographic measuring station Puente Angostura, near the outflow point of the Orinoco River, reasonably well. This judgement was based on calibration and extensive verification of the model for this measuring station. During verification the model also proved to be able to simulate monthly discharge quite well for some measuring stations upstream of Puente Angostura, but more data is needed to verify this. For the other measuring stations included in this study results were moderate to poor.

Since the developed model proved to be able to simulate monthly discharge at station Puente Angostura reasonably well, the model was considered suitable for predictive simulations of scenarios of human interventions. Scenario simulation are considered feasible for changes that fall within the range of conditions observed during the time periods used for calibration and verification. Predictions of changes that fall outside this range are more uncertain and should be interpreted with more care.

Scenarios have been made of two human interventions with changes in surface water runoff falling largely within the range of conditions observed during calibration and verification. These interventions were the construction of a dam and diversion of a part of the Orinoco water towards the Rio Negro in the Amazon river basin through a diversion channel. It was shown that the model is able to deal with interventions such as dams and diversions of water to another river basin. The scenarios are only indicative of the possibilities of the model. Therefore the results should be interpreted with great care.

7.2 Recommendations for future model improvements

The model developed may or may not be sufficient for future scenario simulations of human interventions in the Orinoco river basin. Sufficiency depends amongst other things on the type of intervention scenario and the required accuracy needed of the simulation results. Keeping this in mind, a number of more general remarks may be made regarding possible future model improvements.

The present model is based on a rather course raster cell size resolution of approx. 10* 10 km. The coarseness of the resolution may result in significant deviations in river courses and sub catchment boundaries as derived from the Digital Elevation Model (DEM) and the Local Drainage Direction map (LDD) derived from the DEM. Model resolution may be improved by using a hydrologically correct and more detailed digital elevation model (DEM) of the basin, for instance on a 1*1 km raster cell size. It is expected this will significantly increase the accuracy of river courses and delineation of sub basins within the model as compared to the actual real life situation. Better representation of flow paths and sub basin-boundaries is expected to result in a better determination of the water balances of the sub basins of the Orinoco. The model will then better be able to simulate discharge for these sub basins. A hydrologically correct digital elevation model with high detail has recently become available at EROS data centre. This was too late however for implementation in the present model.

When a more detailed resolution for the DEM has been obtained, the verification procedure may be repeated with the resulting new surface water model to determine whether the results have improved. This procedure should be applied especially at stations within sub catchments within the Orinoco basin to see whether the simulated discharges better approach the measured discharges.

The evapotranspiration flux is one of the most significant fluxes in the Orinoco model. Therefore, improvements in the modelling of this flux have high potential for improving the Orinoco model. A land cover map with a classification in which no combinations of land cover types such as ‘forest with pasture’ are included, in combination with crop coefficients that correspond with the distinguished land cover classes on the map may improve results. Furthermore, application of a different and more suitable model for calculation of potential evaporation or reference crop evapotranspiration could improve results.

Other options for improvement to be considered are the timing of the yearly peak discharges and the absolute values of highest and lowest yearly discharges (see chapter 5), in case these will not improve from a more detailed DEM or better evapotranspiration functions. In addition the monthly time step used in the present model may be reconsidered.

The potential field of use of the model as a tool in water management but also in nature management, would expand if the model would become able to simulate flooded areas. Large scale seasonal flooding and inundation are a main characteristic of the Orinoco basin, which is a key process to numerous ecological processes and functions. When this functionality is included the model would, among others, become suitable for hydro-ecological modelling. The effect of human interventions in the river basin through water processes on ecological functions than may be evaluated, after the development of suitable additions to the present model. The relation between river discharge and flooded area may be modelled by developing an empirical relation between them. A main assumption of this method is that the flooded area is mainly determined by river discharge. A series of maps with flooded area and corresponding river discharge data for a considerable time period should be developed in order to find out if this assumption is right and to be able to apply the method.

References

Aerts, J.C.J.H., Kriek, M. and M. Schepel (1998). STREAM (Spatial Tools for River basins and Environment and Analysis of Management options). From: STREAM CD. Delft: Resource Analysis

Anderson, J.R., Hardy, E.E., Roach J.T., and Witmer R.E. (1976). A land use and land cover classification system for use with remote sensor data. United States Geological Survey Professional Paper 964, pp. 28. Washington: United States Government Printing Office.

Batjes, N.H. (1996). Development of a world data set of soil water retention properties using pedotransfer rules. Geoderma 71, pp. 31-52. Amsterdam: Elsevier Science B.V.

Deursen, W.P.A. (1995). Geographical Information Systems and dynamic models. Ph.D. Thesis, Department of Physical Geography, Utrecht University, The Netherlands. Utrecht: Utrecht University.

Deursen, W.P.A. and J.C.J. Kwadijk (1994). The impacts of climate change on the water balance of the Ganges-Brahmaputhra and Yangtze basin. Delft: Resource Analysis.

Doorenbos, J. and W.O. Pruitt (1977). Crop Water Requirements. FAO Irrigation and drainage paper nr. 24. Rome: FAO.

Kwadijk, J.C.J. (1993). The impact of climate change on the discharge of the River Rhine. Ph.D. Thesis, Department of Physical Geography, Utrecht University, The Netherlands. Utrecht: Utrecht University.

MacKee, E.D., Nordin, C.F. and D. Perez-Hernandez (1998). The Waters and Sediments of the Rio Orinoco and its major Tributaries, Venezuela and Colombia. United States Geological Survey water-supply paper, ISSN 0083; 2326/A-B. Washington: United States Government Printing Office.

Meade, R.H., Weibezahn, F.H., Lewis, W.M. and D. Perez-Hernandez (1990). Suspended sediment budget for the Orinoco river. From: Weibezahn, F.H., Haymara, A. and M.W. Lewis (1990). The Orinoco River as an ecosystem. Caracas: Universidad Simon Bolivar.

New, M., Hulme, M. and P. Jones (1998). Representing twentieth century space-time climate variability. Website: http://www.cru.uea.ac.uk.

Perk, M. van der (1996). Muddy Waters. Ph.D. Thesis, Department of Physical Geography, Utrecht University, The Netherlands. Utrecht: Utrecht University.

Rawlins, C.B. (1999). The Orinoco River. New York: Franklin Watts.

Shuttleworth, W.J. (1992). Evaporation. From: Maidment, D.R. (1992). Handbook of Hydrology. New York: McGraw-Hill Publishing Company.

Stallard R.F., Koehnken L. and M.J. Johnsson (1990). Weathering processes and the composition of inorganic material transported through the Orinoco river system, Venezuela and Colombia. From: Weibezahn, F.H., Haymara, A. and M.W. Lewis (1990). The Orinoco River as an ecosystem. Caracas: Universidad Simon Bolivar.

Vonk G.A. (2001). Modelling of dams, reservoirs and floodings in PCRaster, Master Thesis, Department of Environmental Studies and Eco-Hydrology, Faculty of Geographical Sciences, Utrecht University (in prep.).

Ward, R.C. and M. Robinson (2000). Principles of Hydrology. London: McGraw-Hill Publishing Company.

Appendix I: Data Sources and features

Digital elevation model

Dataset:	GTOPO30
Distributer:	USGS EROS Data Center, Sioux Falls, USA
Source:	http://edcdaac.usgs.gov/gtopo30
Projection:	geographic
Resolution:	30 Arc seconds

Land cover map

Dataset:	GLCC version 2.0
Distributer:	USGS EROS Data Center, Sioux Falls, USA
Source:	http://edcdaac.usgs.gov/glcc
Projection:	Lambert-Azimuth equal area
Resolution:	1000m

Map with maximum water storage capacity of the soil

Dataset:	ISRIC-WISE global data set of derived soil properties version 1.0
Distributer:	ISRIC, Wageningen, The Netherlands
Source:	http://www.isric.nl/WISE.htm
Projection:	geographic
Resolution:	0.5 Arc degrees

Meteorological data

Dataset:	CRU Global Climate Dataset version 1.0
Distributer:	Climate Research Unit, University of East Anglia, UK
Source:	Climate Research Unit, University of East Anglia, UK
Projection:	geographic
Resolution:	0.5 Arc degrees

Discharge data

Dataset:	-
Distributer:	The Global Runoff Data Centre, D-56068, Koblenz, Germany
Source:	The Global Runoff Data Centre, D-56068, Koblenz, Germany

Dataset:	-
Distributer:	The Ministerio del Ambiente y de los Recursos Naturales, Venezuela
Source:	The Ministerio del Ambiente y de los Recursos Naturales, Venezuela

Dataset:	-
Distributer:	Instituto de hidrologia meteorologia y estudios ambientales, Colombia
Source:	Instituto de hidrologia meteorologia y estudios ambientales, Colombia

Appendix II : Additional verification results

The graphs in this appendix represent simulated and measured monthly discharge at the measuring stations mentioned in each legend (see figure 2.4). The lower graphs show monthly averaged discharge, the upper show monthly non-averaged discharge.

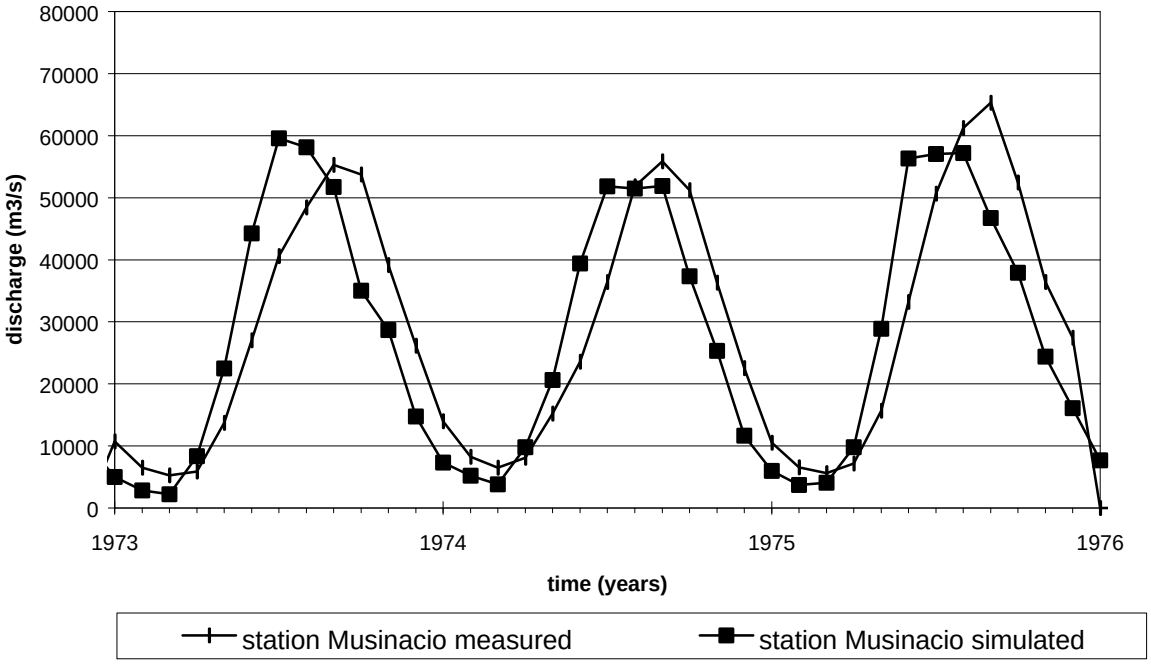

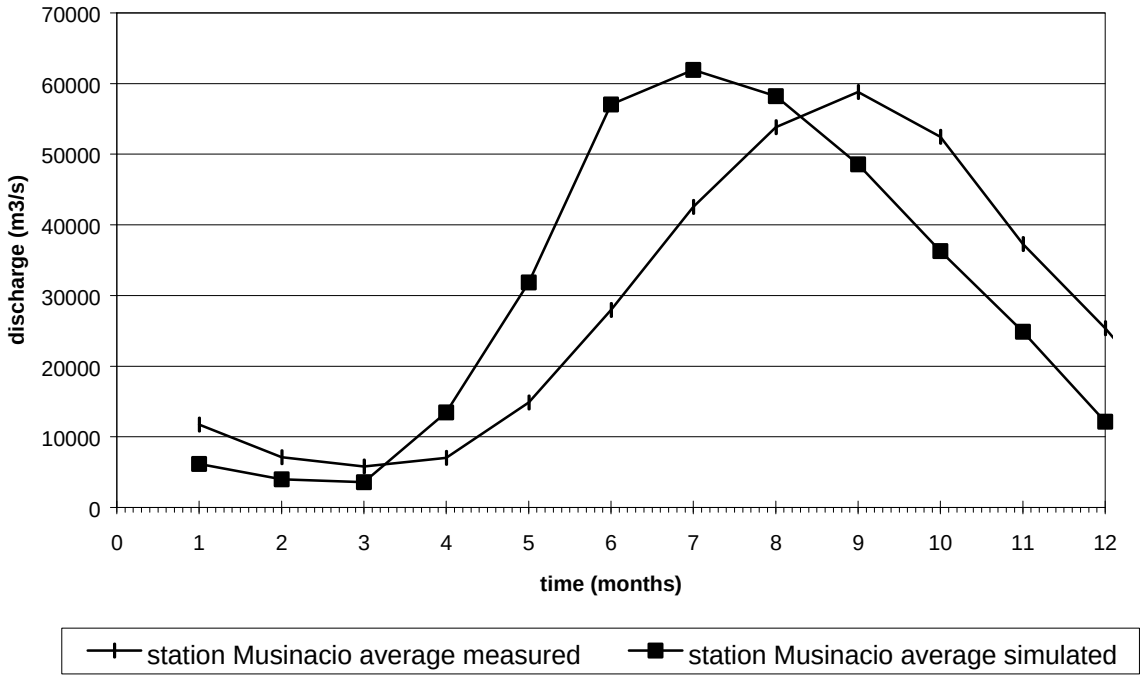

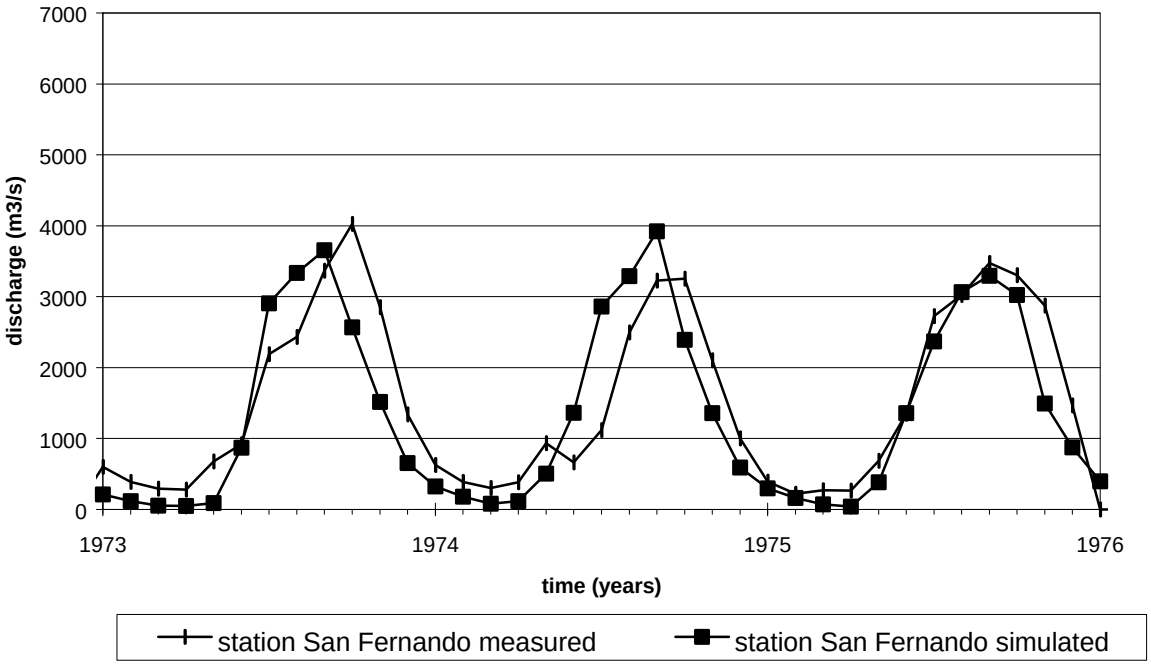
7000
6000
5000
4000
3000
2000
1000
0
discharge (m3/s)
1973
1974
1975
1976
time (years)
station San Fernando measured
station San Fernando simulated

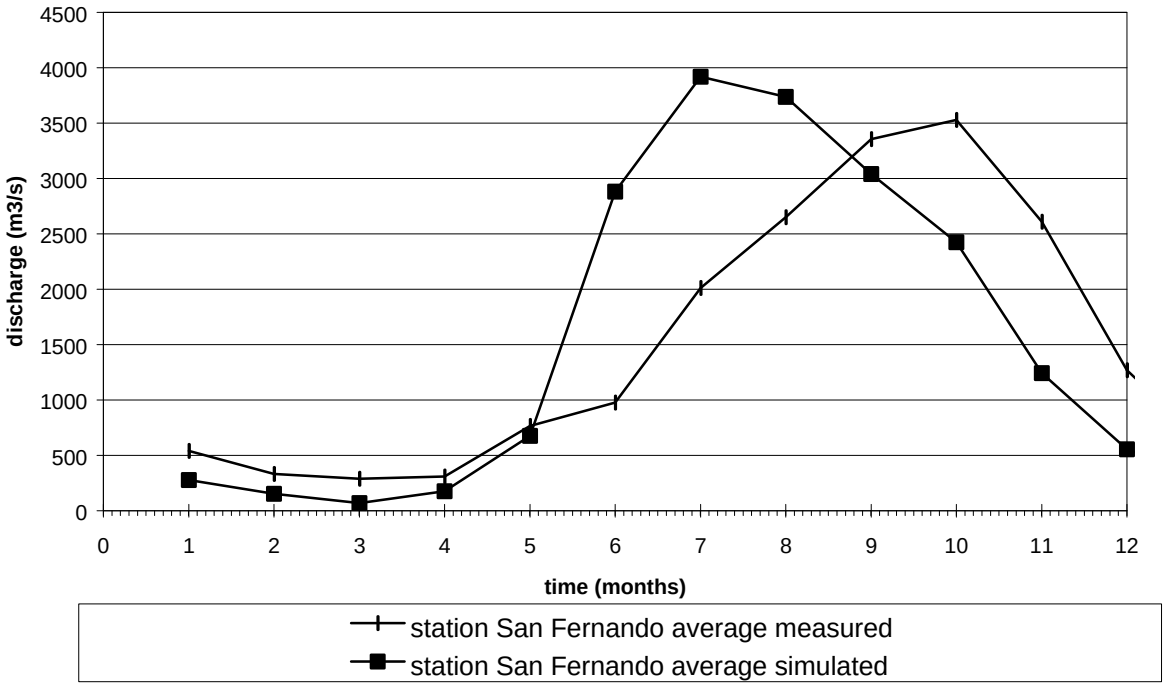
4500
4000
3500
3000
2500
2000
1500
1000
500
0
discharge (m3/s)
0
1
2
3
4
5
6
7
8
9
10
11
12
time (months)
station San Fernando average measured
station San Fernando average simulated

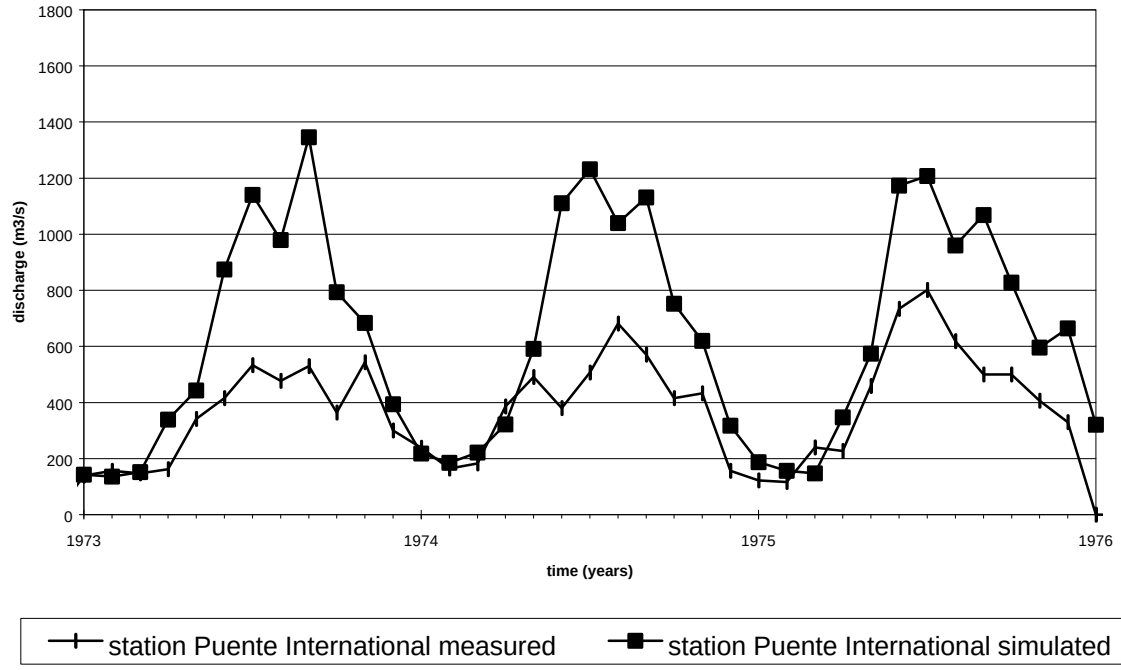

station Puente International measured station Puente International simulated

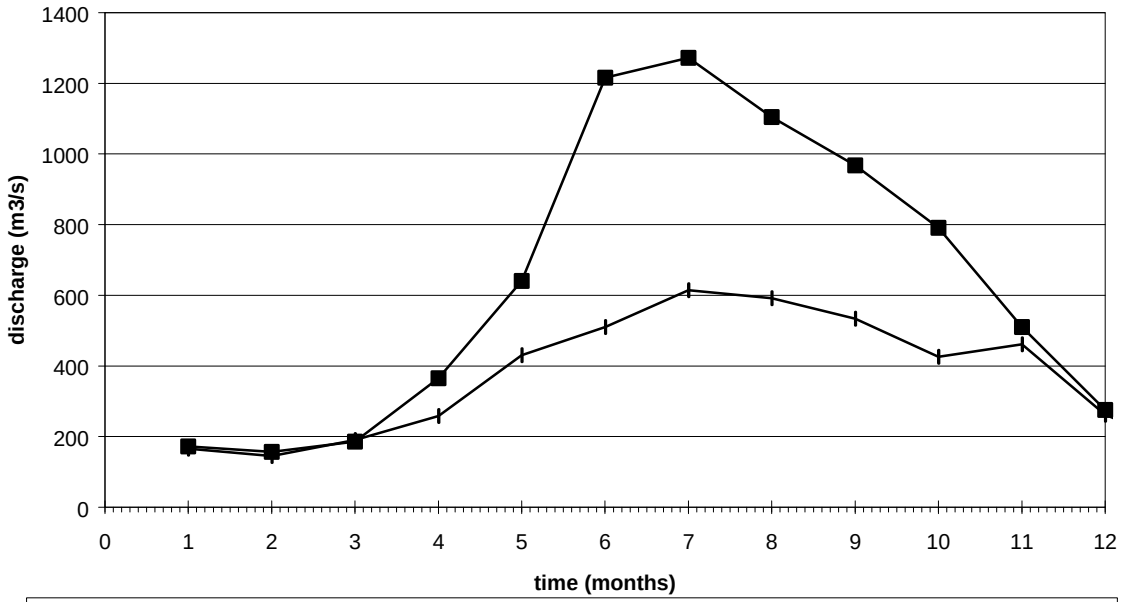

station Puente International average measured
station Puente International average simulated

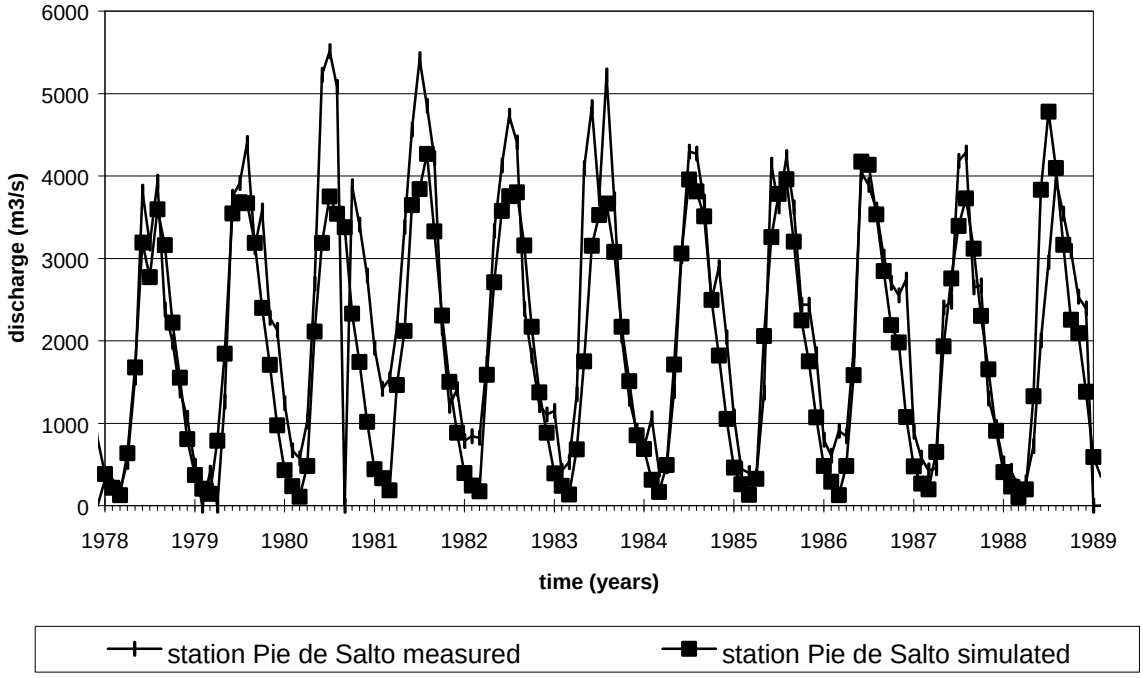
6000
5000
4000
3000
2000
1000
0
discharge (m3/s)
1978
1979
1980
1981
1982
1983
1984
1985
1986
1987
1988
1989
time (years)
station Pie de Salto measured
station Pie de Salto simulated

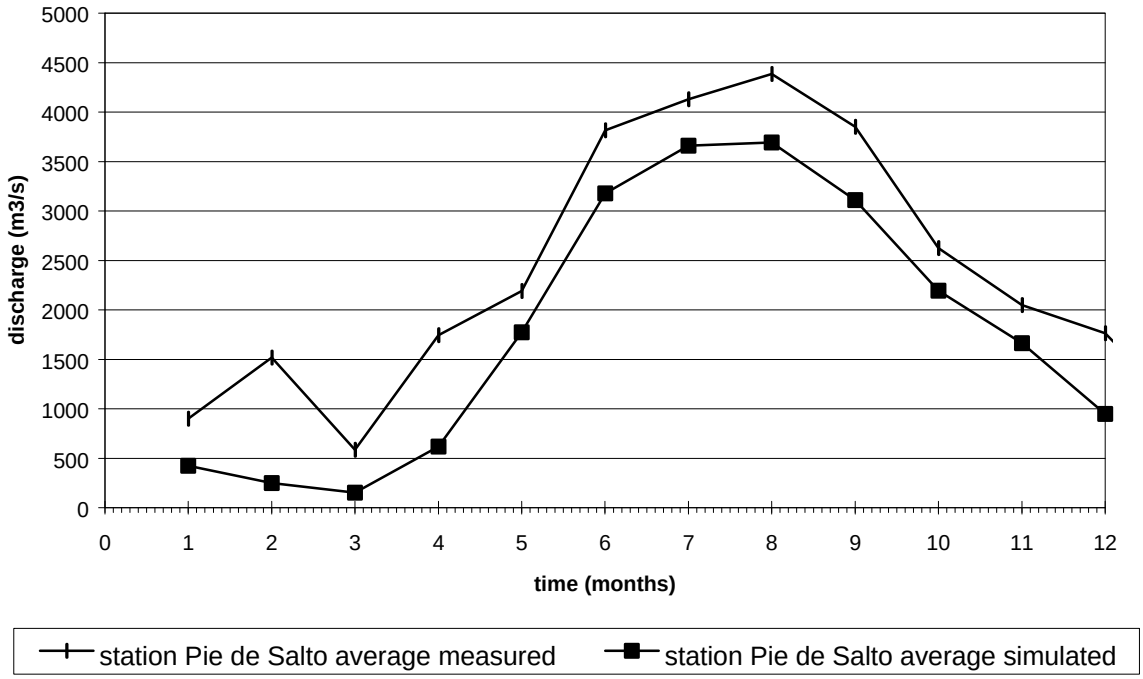
5000
4500
4000
3500
3000
2500
2000
1500
1000
500
0
discharge (m3/s)
0
1
2
3
4
5
6
7
8
9
10
11
12
time (months)
station Pie de Salto average measured
station Pie de Salto average simulated

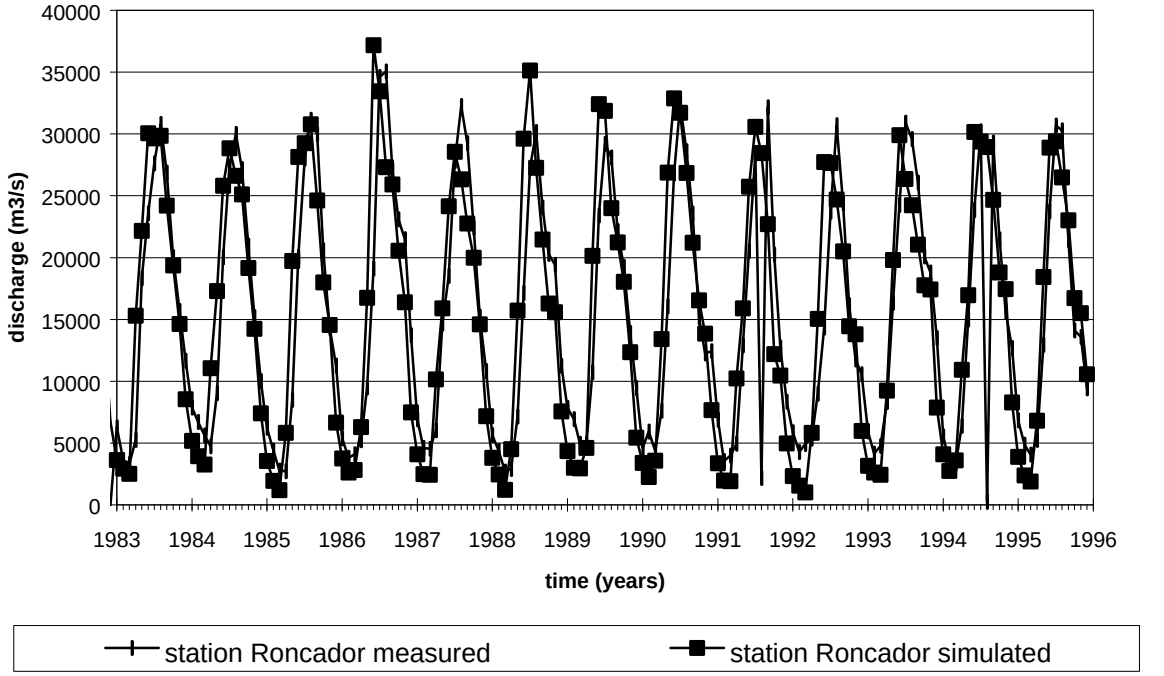
40000
35000
30000
25000
20000
15000
10000
5000
0
discharge (m3/s)
1983
1984
1985
1986
1987
1988
1989
1990
1991
1992
1993
1994
1995
1996
time (years)
station Roncador measured
station Roncador simulated

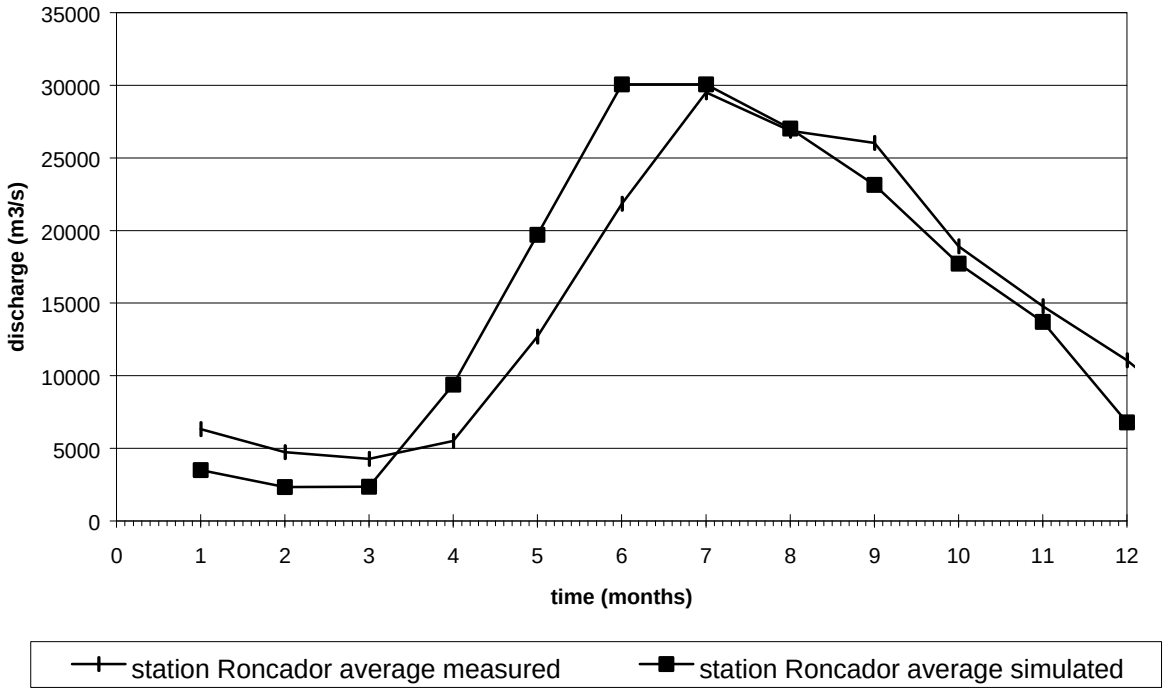
35000
30000
25000
20000
15000
10000
5000
0
discharge (m3/s)
0
1
2
3
4
5
6
7
8
9
10
11
12
time (months)
station Roncador average measured
station Roncador average simulated

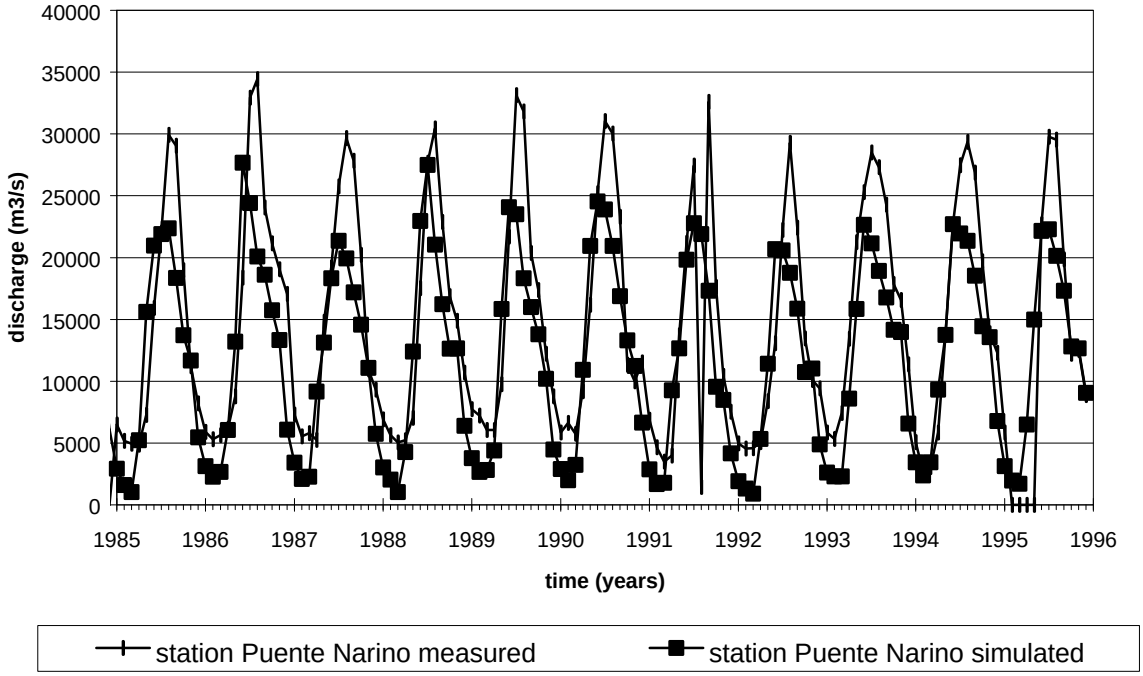
40000
35000
30000
25000
20000
15000
10000
5000
0
discharge (m3/s)
1985
1986
1987
1988
1989
1990
1991
1992
1993
1994
1995
1996
time (years)
station Puente Narino measured
station Puente Narino simulated

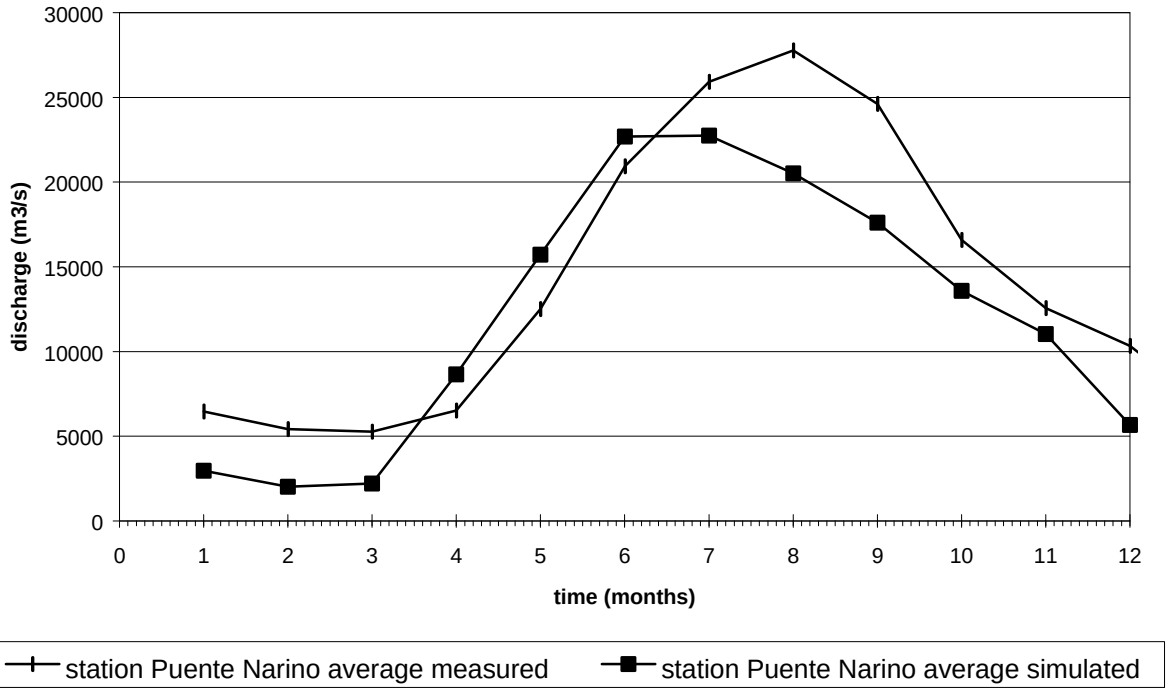
30000
25000
20000
15000
10000
5000
0
discharge (m3/s)
0
1
2
3
4
5
6
7
8
9
10
11
12
time (months)
station Puente Narino average measured
station Puente Narino average simulated

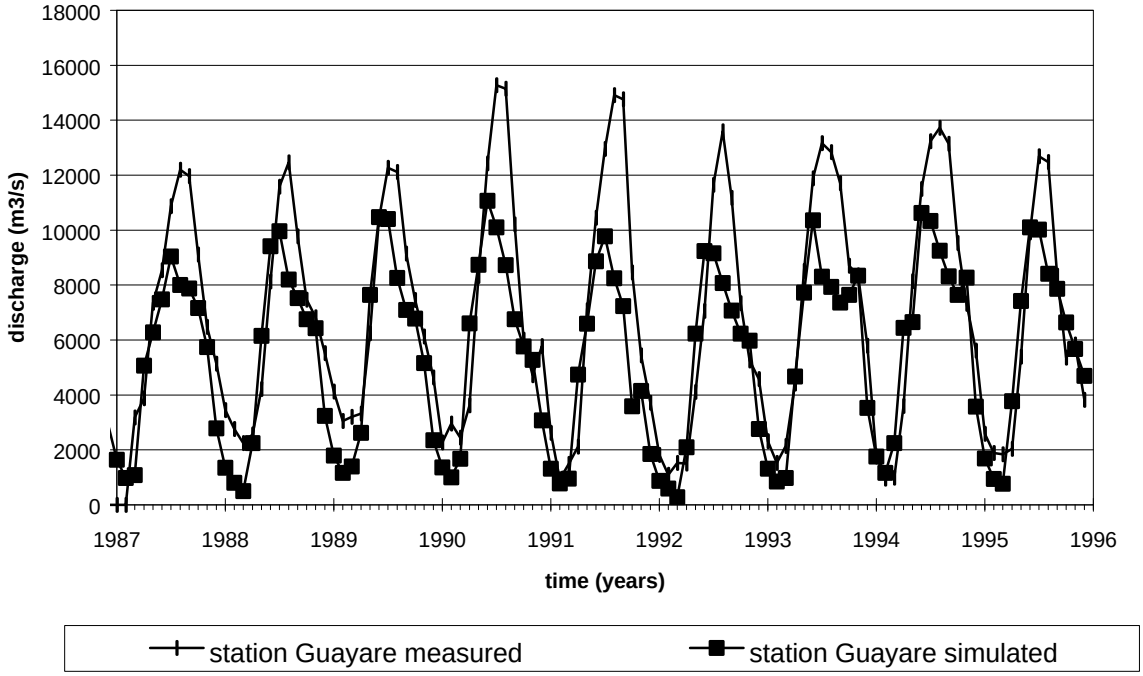
18000
16000
14000
12000
10000
8000
6000
4000
2000
0
discharge (m3/s)
1987
1988
1989
1990
1991
1992
1993
1994
1995
1996
time (years)
station Guayare measured
station Guayare simulated

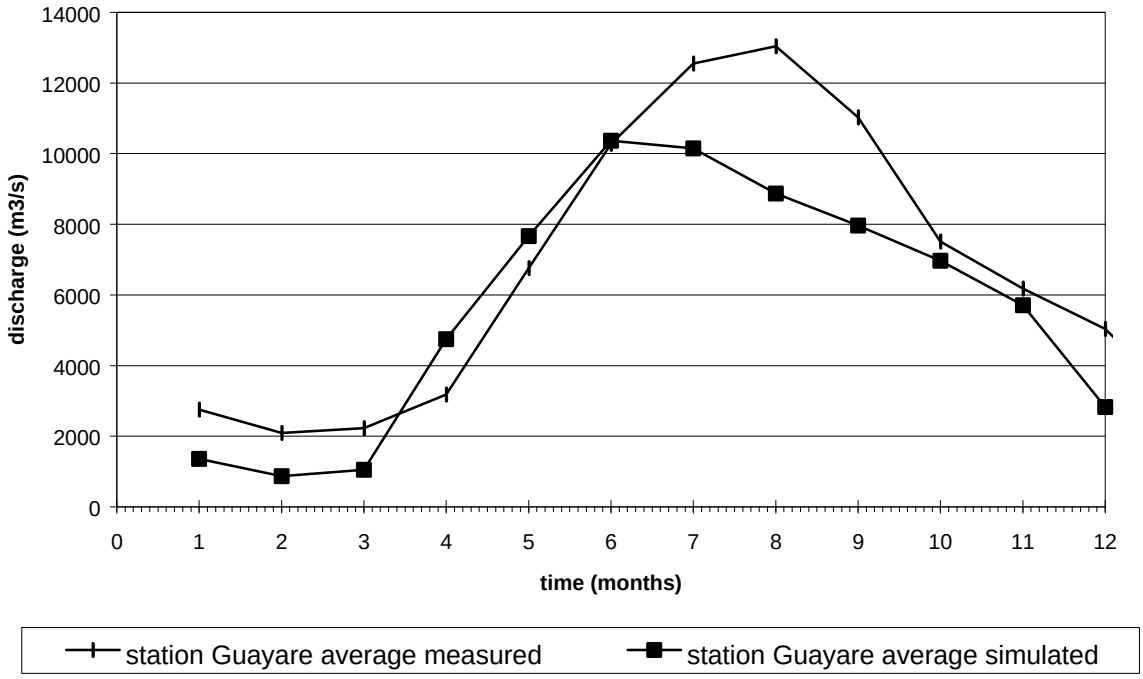
14000
12000
10000
8000
6000
4000
2000
0
discharge (m3/s)
0
1
2
3
4
5
6
7
8
9
10
11
12
time (months)
station Guayare average measured
station Guayare average simulated

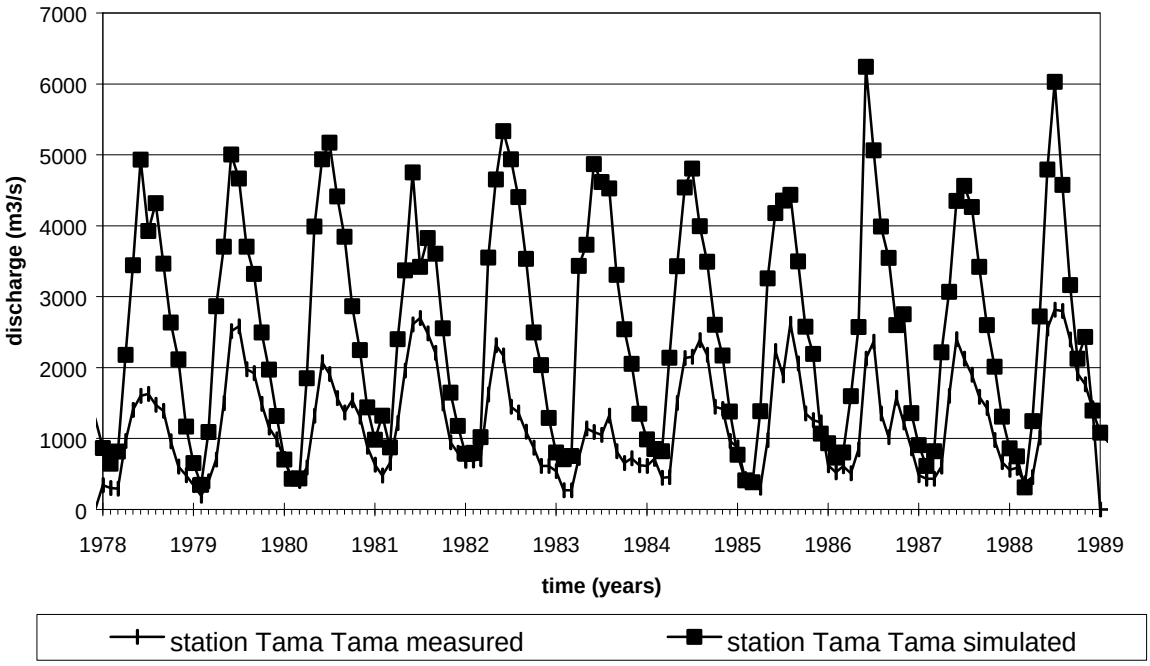
7000
6000
5000
4000
3000
2000
1000
0
discharge (m3/s)
1978
1979
1980
1981
1982
1983
1984
1985
1986
1987
1988
1989
time (years)
station Tama Tama measured
station Tama Tama simulated

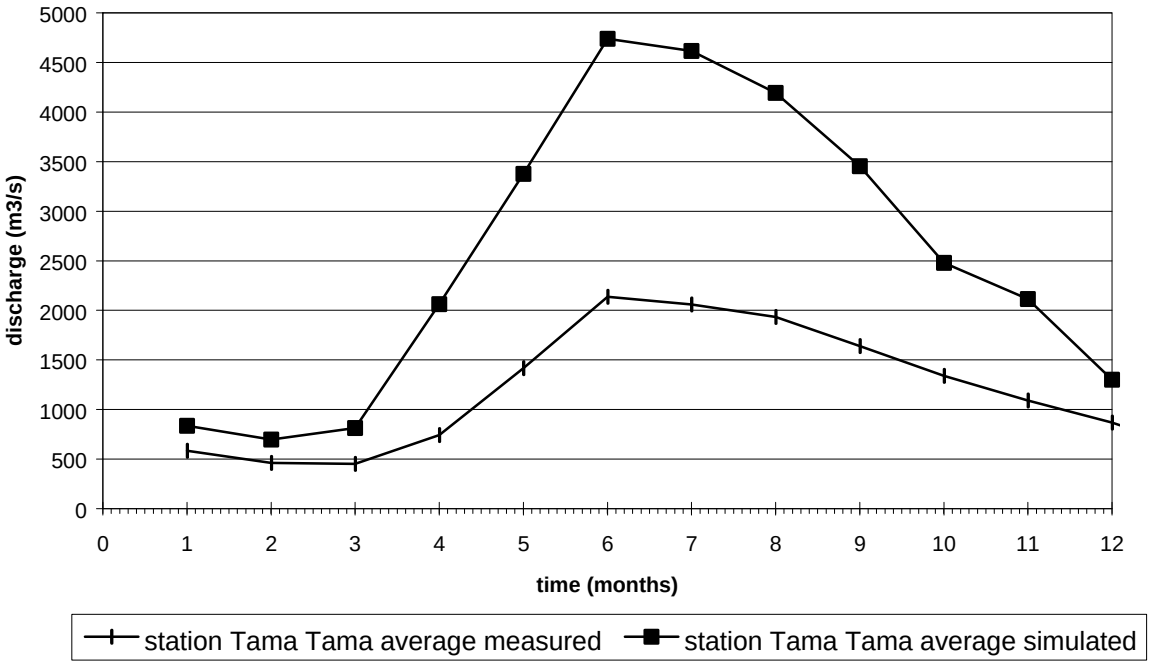
5000
4500
4000
3500
3000
2500
2000
1500
1000
500
0
discharge (m3/s)
0
1
2
3
4
5
6
7
8
9
10
11
12
time (months)
station Tama Tama average measured
station Tama Tama average simulated